THE AMERICAN MINERALOGIST

JOURNAL OF THE MINERALOGICAL SOCIETY OF AMERICA

Vol. 28 JULY–AUGUST, 1943 Nos. 7 and 8

THE CRYSTALLOGRAPHY OF ACANTHITE, Ag_2S

Lewis S. Ramsdell, *University of Michigan, Ann Arbor, Michigan.*

Abstract

An x-ray investigation of acanthite indicates a monoclinic unit cell, with $a=9.47$Å, $b=6.92$Å, $c=8.28$Å, and $\beta=124°$. The probable space group is $B2_1/c$. The unit cell contains 8 Ag_2S. Polysynthetic twinning parallel to (001) and contact twinning parallel to (100) were both found. The observed cell dimensions and the twinning are such that the monoclinic symmetry is readily reconciled with the previous assignment of acanthite to the orthorhombic and to the cubic systems.

Introduction

Silver sulfide, Ag_2S, is dimorphous, occurring in a high-temperature cubic modification known as argentite, and in a low-temperature form, acanthite. Acanthite has usually been considered to be orthorhombic and the axial ratio in common use is that of Dauber (1857), with $a:b:c=0.6886:1:0.9944$. The close approach of its interfacial angles to those characteristic of the cubic system has led some, including Krenner (1888), to regard acanthite as merely a distorted form of argentite. On the other hand, Groth (1878) described crystals from Annaberg, Saxony, which showed marked monoclinic symmetry. Several of the drawings of acanthite in Goldschmidt's *Atlas der Kristallformen* likewise are distinctly monoclinic in appearance.

It was pointed out by the author (1925, 1927) that powder photographs of Ag_2S indicate that at ordinary temperatures only the non-cubic modification exists, and that all cubic "crystals" of argentite are in reality acanthite paramorphs after argentite. Powder photographs of synthetic Ag_2S gave a pattern identical with that obtained from the natural minerals. No attempt was made to interpret this pattern. Emmons, Stockwell and Jones (1926) made powder photographs above 180°C. and obtained a pattern for the cubic form.

Palacios and Salvia (1931) made both powder photographs and spectrographic measurements from the cube face of an argentite "crystal." From the latter they obtained a "split" reflection, the two parts corresponding to interplanar spacings of 2.45 and 2.39Å, respectively. They correlated the first value with a cubic lattice, and assumed that the second pertained to the orthorhombic modification. Their powder photograph pattern consisted of 32 lines. Considering the above value of 2.45Å to be d_{200}, thirteen of their powder photograph lines were interpreted as cubic. These were believed to be characteristic of a Cu_2O-type of structure. The remaining lines of the powder photograph were assumed to belong to an orthorhombic unit cell, whose dimensions were obtained by combining the above value of 2.39Å, considered to be d_{200}, with the orthorhombic axial ratio. However, these remaining lines were not indexed. Identical patterns were obtained from argentite, acanthite and artificial material. Thus according to their interpretation both the high and the low temperature modifications are present in all samples at room temperature.

DESCRIPTION OF SPECIMENS USED

Two types of acanthite crystals were used for the x-ray investigation. Type 1 consists of very slender crystals from Porco, Bolivia; U. S. National Museum No. C-402. The writer wishes to take this opportunity to acknowledge the kindness of Dr. W. F. Foshag of the National Museum in making available this specimen. The crystals used are several millimeters in length, and from 0.2 to 0.3 mm. across. They consist of a nearly square prism, truncated by one main terminal face (Fig. 1*a*). This face has a value for ρ of about 36°, and is located over the intersection of two prism faces. There appears to be a plane of symmetry bisecting this terminal face, and the combination suggests a monoclinic prism with either a basal pinacoid or a hemi-orthodome.[1] A few minute and imperfect faces are present in addition to these larger faces. In general the reflections obtained on the optical goniometer were of fair quality.

Type 2 is represented by a specimen from Himmelsfürst, near Freiberg, Saxony. Dauber made his axial ratio measurements on crystals from this locality, and the majority of the crystals pictured in Goldschmidt's *Atlas der Kristallformen* are likewise from there. From this Himmelsfürst specimen there was obtained a crystal much larger than those of type 1, being nearly 2 cm. in length, and about 1.5 mm. in greatest width. This crystal has been bent nearly at right angles, but fortunately near the tip there is a straight undistorted portion. The cross section is rectangular, and on the two opposite narrow faces there is a herring-bone pattern of striations, suggesting contact twinning (Fig. 1*c*). The crystal is tapered at the end, but the terminal faces are indistinct. In general appearance it is somewhat like Nos. 37 and 43 in Goldschmidt's *Atlas*. Out of the 46 drawings of acanthite crystals in the *Atlas*, there is nothing corresponding to the type 1 crystals.

---

[1] The interfacial angles are such that they are very close to those of a cubic combination consisting of four vertical cube faces, truncated by a 112 face.

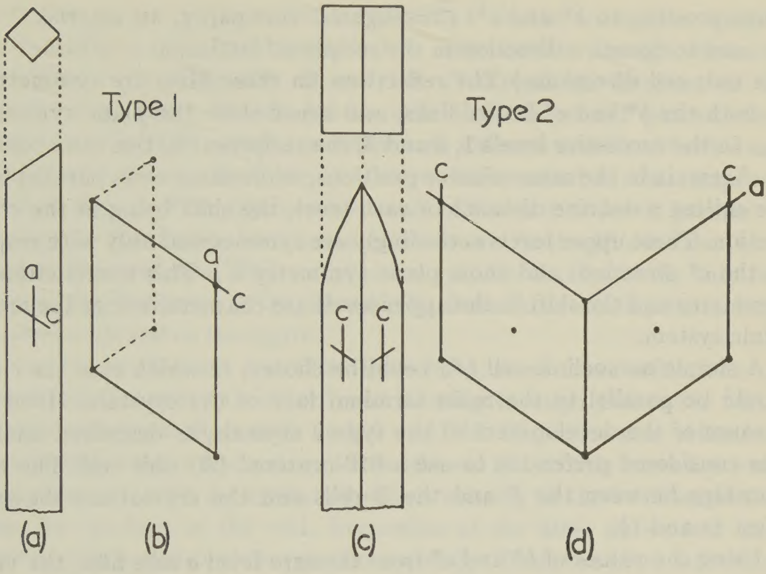

FIG. 1. Relationship of type 1 and type 2 crystals to the unit cell.
(a) Type 1 crystal.
(b) Unit cells: 010-centered (*B*) cell, solid lines; simple (*P*) cell, dashed lines.
(c) Type 2 crystal, showing contact twinning.
(d) Two B cells in twinned position as found in type 2.

X-RAY INVESTIGATION. TYPE 1 CRYSTALS

The crystals were assumed to be monoclinic, and the direction perpendicular to the symmetry plane was therefore chosen as the *b* axis. If the convention $c<a$ is observed, the direction of elongation is the *a* axis. This is in contrast to the type 2 crystal, which is elongated parallel to *c*. Rotation photographs, and zero, first, second and third level equi-inclination Weissenberg photographs were obtained about the *a* axis. From the rotation photographs the value of the identity period along the *a* axis was determined to be about 9.50Å.

The quality of the Weissenberg photographs varies greatly, some being excellent and others poor. This is chiefly due to the high absorption by Ag_2S of the CuK_α radiation used. Some areas of the films have large numbers of reflections clearly recorded, while adjacent areas may be practically blank. In general the reflections are sharp, showing that in spite of the ease with which the crystals may be distorted, no such distortion has occurred.

Zero level films about the *a* axis were obtained from three different crystals of type 1. These all show two central lattice lines 90° apart, corresponding to b^* and c^*. (Throughout this paper, an asterisk * will be used to denote a direction in the reciprocal lattice, as contrasted with the unit cell directions.) The reflections on these films are symmetrical to both the b^* and c^* lattice lines, and hence show the plane symmetry C_{2l}. In the successive levels 1, 2 and 3, the reciprocal lattice rows parallel to c^* remain in the same relative positions, while those rows parallel to b^* are shifted a definite distance in each level, the shift being in the c^* direction. These upper levels accordingly are symmetrical only with respect to the c^* direction, and show plane symmetry C_l. This combination of symmetry and the shift in the upper levels are characteristic of the monoclinic system.

A simple monoclinic cell (*P*) could be chosen, in which case the *c* axis would be parallel to the main terminal face of the crystals. However, because of the development of the type 2 crystals, as described later, it was considered preferable to use a 010-centered (*B*) unit cell. The relationships between the *P* and the *B* cells and the crystal are shown in Figs. 1*a* and 1*b*.

Using the values of b^* and c^* from the zero level *a* axis film, the value of *a* from the rotation photograph, and the value of a^* as subsequently determined from the *b* axis films, the following dimensions are obtained for this *B* unit cell:

$$a = 9.47\text{Å}$$
$$b = 6.92$$
$$c = 8.28$$
$$\beta = 124°$$

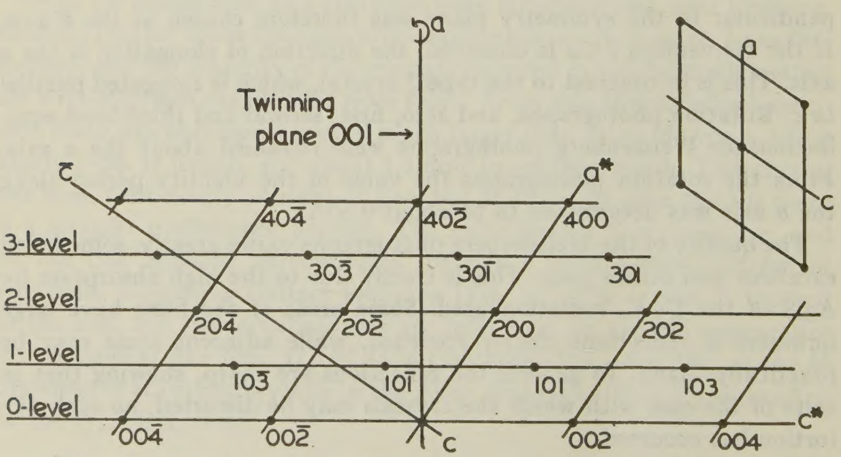

FIG. 2. Cross section through reciprocal lattice, showing sequence of levels in the a^*–c^* plane. Rotation axis is *a*.

The sequence of lattice rows parallel to c^* in the successive levels is shown in Fig. 2. This figure represents a cross section through the reciprocal lattice including the a^* and the c^* directions. Because of the 010-centering, there should be no reflections from ***hkl*** planes when $h+l\neq 2n$, or in other words, no reflections unless h and l are both even, or both odd. Such points are the only ones marked in the reciprocal lattice in Fig. 2. This applies also to all of the lattice levels parallel to the plane of the figure, for all successive levels in the b^* direction have identical patterns, and differ only in the value of k. Hence the only lattice rows perpendicular to the plane of Fig. 2 are those which pass through the points marked in the figure.

Actually, on the first and third level films, some extra reflections are present which appear to be on rows passing through points for which $h+l\neq 2n$, having indices such as $1k2$ and $3k2$. No such extra reflections are to be observed in the zero and second level films. This is not a normal set of absences, with $h+l\neq 2n$ reflections missing in the even numbered levels, but present in the odd. Inspection of the films shows two facts which furnish a clue to this apparent anomaly. First, the extra reflections on the odd level films are not precisely half-way between the rows for which $h+l=2n$. Second, these extra reflections are fairly weak, and in every case are located symmetrically across the central lattice line parallel to b^*, with respect to intense reflections of the $h+l=2n$ type. In the monoclinic system such symmetry should not be present.

This pseudo-symmetry, with strong reflections appearing mirrored across the (001) plane, must be due to twinning parallel to (001). This twinning is probably microscopic, for there is no visible external evidence of twinning. The fact that only strong reflections are thus repeated suggests that the greater part of the crystal consists of one orientation, with the reversed twinned position making up only a small portion and therefore contributing little to the reflections.

The fact that these extra spots resulting from twinning apparently fit into the regular sequence of reflections in the odd levels and are missing in the second level is due entirely to a fortuitous situation, arising from the particular values of a, c and β existing in the structure. This can be seen from Fig. 2, in which the rotation axis a represents the trace of the twinning plane. The effect of the twinning is to reflect all lattice points on one side of the plane to symmetrical positions on the other. Thus in the zero level all points $0k\bar{l}$ are mirrored across the twin plane and coincide with identical $0kl$ points, so that there is no effect observable. In the first level, the point $10\bar{1}$ is reflected across the twin plane and appears almost exactly at the position where 100 would be, if present. Likewise $10\bar{3}$ in the twinned position appears where 102 would be. In general, the lattice rows $1k\bar{1}$ and $1k\bar{3}$ from one portion of the twin appear in the positions $1k0$ and $1k2$, respectively, of the other. Thus legitimate reflections $(h+l=2n)$ from one twin orientation appear approximately in forbidden positions $(h+l\neq 2n)$ of the other.

A different situation exists in the second level. Here $20\bar{2}$ is reflected across the twin plane and practically coincides with 200, and $20\bar{4}$ with 202, etc. Or in general, lattice rows $2k\bar{2}$ and $2k\bar{4}$ when reflected practically coincide with the rows $2k0$ and $2k2$, respectively. A careful inspection of the second level films reveals that some of the spots are doublets. This doubling is due to the lack of exact coincidence between the position of a given reflection from one part of the twin and that of the extra one from the other. Not all spots show this doubling, because one or the other of the two possibilities may be absent. If only a single spot occurs, there may be doubt as to its identity, but since both possible reflections belong to the category of $h+l=2n$, there is no ambiguity about the type of missing reflections. The degree of coincidence of pairs of reflections from the two parts of the twin decreases with decreasing interplanar spacing, or, in terms of the reciprocal lattice, decreases with increasing distance from the origin. Consequently the doublets of reflections with high values of θ are clearly separated, and can always be distinguished.

In the third level the situation is similar to that in the first level. Rows in the reciprocal lattice of the type $3k\bar{3}$ and $3k\bar{5}$ (Fig. 2) are mirrored across the twin plane and fall approximately in the positions of $3k0$ and $3k2$, respectively, which are forbidden reflections. However, the degree of approximation is much less, because of the increasing divergence with increasing distance from the origin. On the third level films it is plainly evident that the lattice rows $3k\bar{3}$ and $3k\bar{5}$ in their mirrored positions are not exactly half-way between the adjacent regular rows $3k\bar{1}$, $3k1$ and $3k3$.

The particular values of a, c and β which bring about this situation are such that the lattice is very strongly pseudo-orthorhombic. Thus in Fig. 2 the nearly rectangular block with $40\bar{2}$, 400 and 002 at the corners, and 200 at the center, is clearly apparent.[2] The lattice points outlining all such blocks have both h and l even. The pseudo-symmetry means that for any point of this type there is a corresponding point across the trace of the (001) plane. This corresponding point has different values of h and l, but both are still even. Thus both points of such symmetrical pairs correspond to legitimate reflections. This pseudo-symmetry is so pronounced that two second level films about a, taken 180° apart, appear almost identical. Ordinarily in the monoclinic system two such films would be symmetrical, but not superposable. In this case the shift in successive levels is such that pairs like 200 and 202 are practically equidistant from the rotation axis. In general there is a direct correspondence in position and to a considerable extent a correspondence in intensities on the two films taken 180° apart. This must mean that there is a strong pseudo-symmetry in the atomic positions, at least with respect to the heavier Ag atoms.

---

[2] As will be shown later, this block of the reciprocal lattice is derived from a pseudo-orthorhombic cell, with dimensions in agreement with the usual orthorhombic axial ratio.

In the odd levels, the lattice points have both *h* and *l* odd, and the positions symmetrical to these are unoccupied because they are points with $h+l\neq 2n$. This relationship, and those previously mentioned, are shown in Fig. 3 in terms of the unit cell rather than the reciprocal lattice.

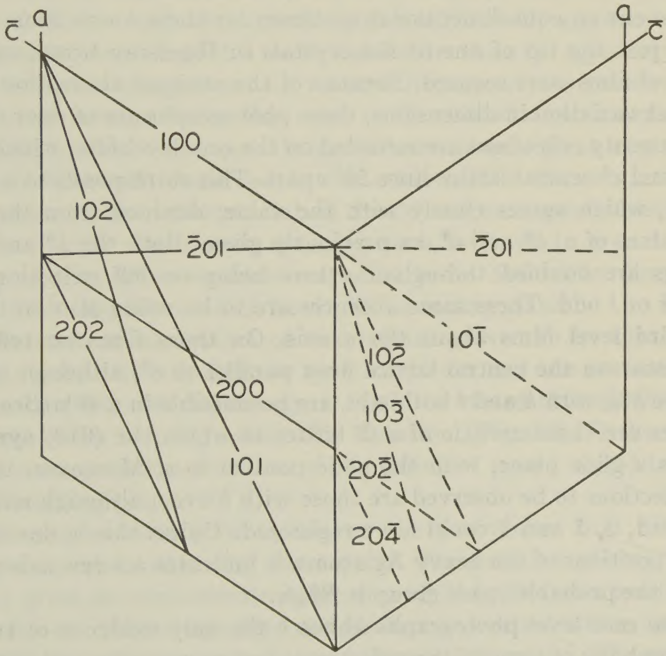

FIG. 3. 010 cross section through twinned *B* cells, showing near parallelism of pairs of planes from the two cells. In pairs such as $10\bar{1}$–100, 101–$10\bar{2}$ and $10\bar{3}$–102 the first member has indices with $h+l=2n$ and the second with $h+l\neq 2n$. The legitimate reflections ($h+l=2n$) from one cell appear in forbidden positions ($h+l\neq 2n$) of the other. Other pairs as 200–$20\bar{2}$ and 202–$20\bar{4}$ have both indices with $h+l=2n$. Note that $\bar{2}01$ is nearly continuous in the two cells.

Planes ***hkl***, with both *h* and *l* even, in one twin orientation are practically parallel to planes ***hkl*** with *h* and *l* even in the other orientation, and have almost the same interplanar spacings. Such pairs are 200-$20\bar{2}$ and 202-$20\bar{4}$. Reflections from such pairs would practically coincide, and hence occur as doublets. But planes *hkl*, with both *h* and *l* odd, in one orientation are practically parallel to planes in the other orientation whose values for *h* and *l* are one odd and one even. Thus 101 is parallel to $10\bar{2}$, $10\bar{3}$ to 102 and $10\bar{1}$ to 100. The second plane of each of these pairs does not reflect in a *B* lattice, but its reflection may be simulated by a reflection from the other twin orientation.

It is thus evident that the assumption of a (001) twinning plane accounts for the presence of doubled reflections, and for the appearance of reflections apparently of the forbidden type, and leaves valid the original choice of a monoclinic *B* cell, with the dimensions stated.

Weissenberg photographs were also taken about the *b* axis of a type 1 crystal. The slender crystals are so easily deformed that no attempt was made to cut an equi-dimensional specimen for these *b* axis films. By inserting just the tip of one of the crystals in the *x*-ray beam, zero and first level films were secured. Because of the unequal absorption due to the great variation in dimensions, these photographs are of poor quality. About twenty reflections are recorded on the zero level film, which shows the a^* and c^* central lattice lines 56° apart. This corresponds to a β angle of 124°, which agrees closely with the value obtained from the measured values of *a*, a^* and c^*, as previously given. Both the a^* and the c^* spacings are doubled throughout, there being no *h*0*l* reflections with either *h* or *l* odd. These same absences are to be noted also on the first and third level films about the *a* axis. On those films no reflections are present on the central lattice lines parallel to c^*, although those of the type *h*0*l*, with *h* and *l* both odd, are permissible in a *B* lattice. These absences are characteristic of a *B* lattice in which the (010) symmetry plane is a glide plane, with the glide parallel to *c*. Moreover, the only 0*k*0 reflections to be observed are those with *k* even, although reflections with $k=1$, 3, 5 and 7 could have registered. Unless this is due to some special positions of the heavy Ag atoms. it indicates a screw axis parallel to *b*, so the probable space group is $B2_1/c$.

In the zero level photographs about *b* the only evidence of twinning is the doubling of some of the reflections, just as was observed in the zero level of the *a* axis films. The absence of all *h*0*l* reflections with either *h* or *l* odd gives no opportunity for the twinning to introduce extra reflections apparently of the forbidden type. In Fig. 2 it will be noticed that the lattice line from the origin through $40\bar{2}$ is very near perpendicular to c^*. On the zero level film this lattice line is doubled, with one strong and one weak reflection, corresponding to the two twin orientations. These reflections are separated by about 1 mm., which represents a divergence of about 2° between the $[40\bar{2}]$ lattice directions in the two parts. This means that the $(20\bar{1})$ planes in the two parts of the twin are within 2° of being parallel. The actual geometrical construction, using the measured values of a, c and β checks this result closely (Fig 3).

The first level films about b are very poor. As would be expected with rotation about the b axis, there is no shift in the relative positions of the lattice rows, and the reflections correspond to the regular (i.e., not doubled) reciprocal lattice spacings. This is because the effect of the glide plane is limited to $h0l$ reflections. Twinning is evidence by the doubling of some spots, and the appearance of some reflections apparently of the $h+l\neq 2n$ type, symmetrically located with respect to reflections in the normal positions.

TYPE 2 CRYSTAL

As previously stated, this crystal is striated in such a manner as to indicate contact twinning. It is much less slender than the type 1 crystals, having a cross section of about 1×1.5 mm. Because of this greater thickness, it would seem probable that most of the reflections obtained would be from the surface. Consequently the reflections on a given area of the film should be chiefly from one or the other half of the contact twin, and the patterns from the two halves should not be blended as they are in the case of the microscopic twinning such as found in type 1. Such blending as does occur would be expected to be limited to film areas close to the b^* direction, which lies in the twinning plane.

The direction of elongation of this crystal proved to be that corresponding to the c direction of the type 1 crystals, and the contact twinning plane is (100). More properly, it might be stated that the B lattice was chosen so as to bring about this situation (Fig. 1*d*). If the simple P lattice were used, the direction of elongation of type 2 would be [102] and the twinning plane $(20\bar{1})$.

The faces gave such poor signals on the goniometer that difficulty was encountered in adjusting the crystal. The rotation photograph is poor, but gives an approximate value of $c=8.24$Å. The zero level Weissenberg film is of better quality, and shows two central lattice lines 90° apart, with the reflections symmetrical about both $-(C_{2l})$. The spacings along these lines agree with those of a^* and b^* as found for type 1. However, this film shows rows of reflections corresponding to $1k0$, $3k0$ and $5k0$, all with $h+l\neq 2n$, in addition to those with $h+l=2n$. The presence of such supposedly forbidden reflections is completely explained by assuming that the same polysynthetic twinning on (001) as found for type 1 is present here, as well as the visible contact twinning on (100).

The relationships involved in this situation are shown in Fig. 4. Like Fig. 2, this is a section through the a^*-c^* plane of the reciprocal lattice, but with the rotation about the c instead of the a axis. The twinning across the (001) plane has the effect of repeating certain lattice rows from one twin orientation in such a way that they appear as rows in the other. The zero level corresponds to the a^*-b^* plane of the reciprocal lattice, being perpendicular to the plane of Fig. 4. Rows of lattice points, likewise perpendicular to the plane of Fig. 4, and represented by the points $\bar{1}01$, $\bar{2}02$, $\bar{3}03$, etc., are repeated across the (001) twin plane and fall almost exactly on the zero level. These appear to be lattice rows passing through the points $\bar{1}00$, $\bar{2}00$, $\bar{3}00$, etc. Half of these, with h even, are legitimate reflections for a B lattice, and cause doubling of spots, since the coincidence is only approximate. The other half, with h odd, will appear as forbidden reflections. Actually, of course, they are legitimate reflections from the other twin orientation.

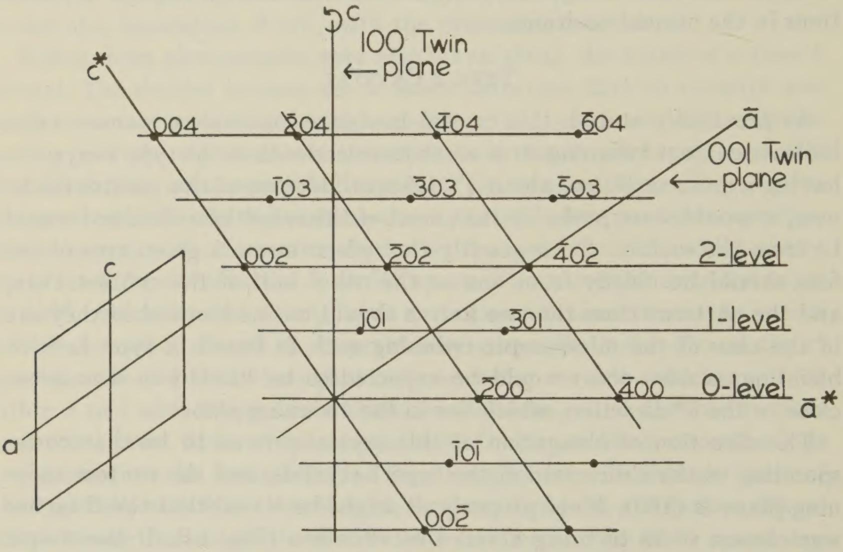

FIG. 4. Cross section through the a^*-c^* plane of the reciprocal lattice. Rotation axis c. Both (001) and (100) twin planes are indicated.

In the first level the only lattice rows in such a position that they could be repeated across the twin plane from the other orientation are all unoccupied. Rows through $\bar{3}02$ and $\bar{4}03$ are examples of this. Accordingly the films for the first level show no extra reflections, either in forbidden positions, or as doublets.

The second level resembles the zero level. Here rows represented by the lattice points $\bar{3}01$, $\bar{2}00$, $\bar{1}0\bar{1}$, $00\bar{2}$, etc., are repeated across the (001) twin plane and fall into positions approximately on the second level. They are able to reflect, and the reflections appear with the normal reflections on the film. Those with *h* even fall on legitimate positions and cause doubling. Those with *h* odd appear as single spots in the forbidden positions $h+l\neq 2n$. These single spots alternate with the doublets. This effect is very noticeable in the second level films, because the divergence is sufficient to make the separation of the doublets appreciable.

This effect is so definitely present that it seems to offer complete verification of the assumption of the polysynthetic twinning across (001), in addition to the contact twinning, (100). Moreover, the effect is continuous over the entire film, for any portion of the crystal giving rise to reflections is made up of both orientations. The contact twinning results in an entirely different appearance. As stated previously, the crystal is of such thickness that the reflections must be chiefly from the surface, and hence the spots registered on any given area of the film in general should be from one half or the other of the twin, without much blending.

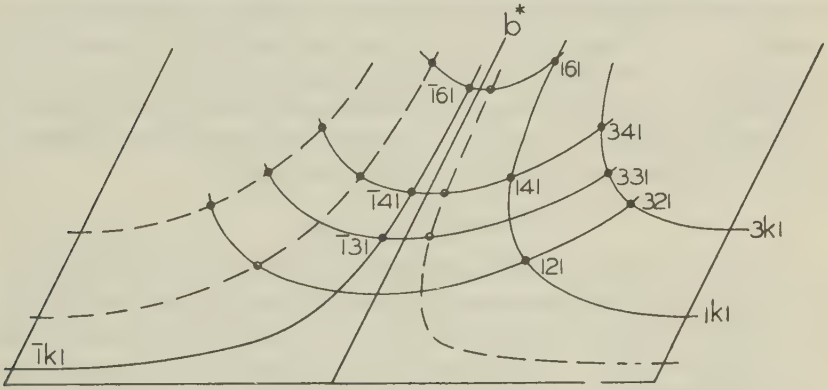

FIG. 5. Diagrammatic representation of 1-level Weissenberg photograph about the *c* axis of type 2 crystal. Solid points represent reflections from one twin (100) orientation; circles represent reflections from the other orientation.

In the zero level, no effect of the contact twinning should be present, and none is apparent on the films. In the first level, however, the shift due to monoclinic symmetry is in opposite directions in the two halves of the twin. The central lattice line parallel to b^* is common to both parts, and on either side of this direction the opposite shifts are symmetrically located. There is little blending of the patterns, for only a few reflections from one half persist across the central lattice line into the domain of the other. The appearance of the film is shown diagrammatically in Fig. 5. As stated previously, no effect of the (001) twinning is evident in the first level, so there are no doublets nor reflections apparently in forbidden positions. However, both of these effects again appear in the second level films, together with the effect of the contact twinning. This latter consists of the symmetrical shifting of the lattice rows in opposite directions on either side of the central lattice line parallel to b^*, with a few reflections from one orientation appearing on the opposite side.

LAUE PHOTOGRAPHS

Laue photographs of type 1 crystals were taken perpendicular to (001) and (010). The former shows the (010) symmetry plane, and a suggestion of symmetry across the trace of the (100) plane. If both orientations of the polysynthetic twinning were present in equal proportions, the reflections should appear entirely symmetrical across the (100) plane. Preponderance of one orientation, such as was indicated by the Weissenberg photographs, is revealed in the Laue photographs by the lack of this apparent symmetry. Likewise, the photograph perpendicular to (010), although showing many reflections symmetrical to both (100) and (001), actually possesses only a two-fold axis of symmetry.

POWDER PHOTOGRAPHS

Different specimens of Ag_2S gave widely varying qualities of powder photographs. The best film obtained was made with MoK_α radiation in a camera with an eight inch radius. The shorter wave-length resulted in more reflections, and the large radius was sufficient to resolve pairs of lines that appeared as single lines with a smaller camera, even when using CuK_α radiation. A composite list of reflections with their estimated intensities, together with the assigned indices are given in Table 1. The values was obtained are in good agreement with those given by Harcourt (1942). Some of the powder photograph data of Palacios and Salvia are included in the table.

TABLE 1

This table gives the spacings as determined from the powder photographs; the observed intensities, with the strongest lines rated as 10; the monoclinic indices *hkl*; the spacings as calculated for the monoclinic unit; and the intensities of the corresponding reflections as observed on the Weissenberg photographs.

d Å	*I* obs.	Mono. *hkl*	*d* calcd.	*I* Weiss.
3.91	1	200	3.92	m
		$20\bar{2}$	3.87	s
3.40	7	002	3.43	m
		210	3.41	ms
		$21\bar{2}$	3.37	m
3.07	8	012	3.075	m
2.81	8	$31\bar{1}$	2.81	s
2.66[3]	6	121	2.655	s
2.58[3]	10	220	2.595	ms
		$22\bar{2}$	2.578	m
2.44	10	$11\bar{3}$	2.453	m
		022	2.435	vs
		$31\bar{3}$	2.415	ms
2.37	9	$40\bar{2}$	2.36	s
2.315[2]	a			
2.205	7	$13\bar{1}$	2.21	ms
2.08	8	$12\bar{3}$	2.09	ms
		202	2.07	m
2.05	4	$32\bar{3}$	2.065	ms
		$20\bar{4}$	2.045	m
1.99	4	230	1.988	w
		212	1.984	m
		$23\bar{2}$	1.981	w
1.96	5	$21\bar{4}$	1.962	m
		400	1.96	w
1.51	4	$34\bar{1}$	1.507	w
1.475	3	133	1.477	s
1.46	5	$11\bar{5}$	1.467	m
1.44	4	$14\bar{3}$	1.444	m
		$34\bar{3}$	1.435	w
1.41	<1	$62\bar{2}$	1.407	m
1.38	<1	034	1.376	vw
1.335	2	$33\bar{5}$	1.343	ms
(broad)		341	1.331	w
		341	1.331	w
		242	1.328	m
		204	1.32	w
1.30	1	600	1.31	w
		250	1.305	w
		214	1.30	w
		422	1.296	m
		440	1.296	w
		$60\bar{6}$	1.29	m
		052	1.285	m
1.265	1	323	1.27	w
		$35\bar{1}$	1.26	m
1.23	3	224	1.236	w
(broad)		$22\bar{6}$	1.228	w
		$15\bar{3}$	1.223	m
		115	1.22	w
		044	1.218	m
1.18	<1	333	1.185	m
		804	1.18	w
1.155	<1	060	1.15	m
		252	1.15	w

TABLE 1—*continued*

d Å	*I* obs.	Mono. *hkl*	*d* calcd.	*I* Weiss.	*d* Å	*I* obs.	Mono. *hkl*	*d* calcd.	*I* Weiss.
1.905	4	032	1.914	m			234	1.15	m
		410	1.885	w			25$\bar{4}$	1.145	w
1.865	4	41$\bar{4}$	1.86	m	1.13	<1	016	1.13	w
1.72	7	13$\bar{3}$	1.732	vw	1.09	<1	062	1.092	m
		040	1.73	m			135	1.091	mw
		33$\bar{3}$	1.717	w					
					1.08[2]	a			
1.68[1]	a								
1.60[2]	a				1.04	<1	337	1.03	w
1.58	5	240	1.595	mw	1.01	<1	262	1.01	m
		24$\bar{2}$	1.579	mw			361	1.01	w
1.54	4	331	1.546	m	.965	<1	800	.98	m
		042	1.545	m			254	.965	w
		232	1.541	w					
		024	1.537	m					
					.94	<1	216	.95	w
							226	.93	w

---

[1] This line was the only one listed by Palacios and Salvia as strong, but does not appear on any of the author's films.

[2] These lines were reported as weak by Palacios and Salvia, but were not observed by the author.

[3] Both Harcourt and Palacios and Salvia report these two lines as one strong line, but on the author's films they are clearly separated.

CORRELATION OF THE MONOCLINIC SYMMETRY WITH PREVIOUS ASSIGNMENTS TO THE ORTHORHOMBIC AND CUBIC SYSTEMS

If the low temperature form of Ag_2S is monoclinic, there arises the problem of reconciling this fact with the *x*-ray data of Palacios and Salvia, and with the morphological data in the literature, which refer acanthite both to the orthorhombic and the cubic systems.

With one exception there is good agreement between the positions of the powder photograph lines of the author and those of Palacios and Salvia. They list 32 lines, three of which, of low intensity, were not observed on the author's films. On the other hand, their list of 32 did not include eight which were found by the author. Moreover, they rated only one line (1.68Å) as having a strong intensity, and this line was not found on any of the author's films, nor does it appear in the list given by Harcourt. In addition to this discrepancy, there are some differences in the estimated intensities of certain of the lines. All of the powder photograph lines are listed in Table 1.

The erroneous interpretation of acanthite as orthorhombic is due to the fact that the monoclinic cell is pseudo-orthorhombic. Figure 6 shows this relationship. The commonly accepted axial ratio for acanthite applies to this pseudo-cell. Palacios and Salvia obtained their unit cell dimensions by combining an accidentally correct value for d_{200} with the axial ratio, and hence their figures are in agreement. They give 4.77Å as the length of *a*, which value is almost exactly one-half of *a* in the monoclinic cell, 9.47Å. Their value for *c*, 6.88Å, checks closely with that of 6.86Å for d_{001} in the monoclinic unit, while the two values for *b* are the same, 6.92Å.

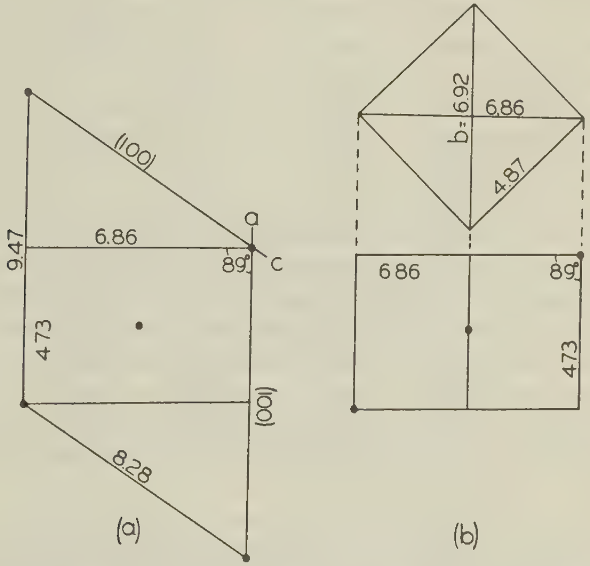

FIG. 6. (a) Cross section through *B* cell, showing relation to pseudo-orthorhombic unit. (b) Diagram showing relation of pseudo-orthorhombic unit to the pseudo-cubic unit.

It must be noted, however, that this orthorhombic unit is not a true unit cell, for only half of the lattice corners are occupied, and only every other unit has the *B*-centered lattice position. Moreover, as shown in Fig. 6, the orthorhombic unit is not truly orthogonal, the angle between (100) and (001) being approximately 89°. The correspondence between the two cells is so close, however, that any *h'k'l'* plane in the orthorhombic cell can be given monoclinic indices *hkl*, and the spacings calculated for such a unit on the basis of an orthogonal cell will agree with the actual spacings practically within the limits of error in measurement.

However, the monoclinic lattice has certain spacings which have no direct counterpart when referred to the orthorhombic lattice. They are just twice as great as the orthorhombic spacings should be. This is because the orthorhombic cell is a fictitious one, with some of the lattice points missing. Every real plane, of course, must pass through lattice points. In the case of the orthorhombic lattice, there are certain families of planes such that every other plane passes through occupied lattice points, while the planes in between pass only through the unoccupied points, and hence are fictitious planes. In these cases the actual interplanar spacing is just twice what it would be in a normal lattice. This is illustrated by the monoclinic plane $31\bar{1}$, which is parallel to 321 in the orthorhombic, but whose spacing is $2\times d_{321}$. A direct, but possibly unorthodox way in which such a sequence of spacings can be given Miller indices is by using fractions.[3] Likewise the transformation formula must use fractions to express this relationship properly. The transformation formula for monoclinic to orthorhombic is $\frac{1}{2}00/010/\frac{1}{2}01$. Using this formula, the above mentioned monoclinic plane $31\bar{1}$ transforms to $\frac{3}{2}\ 1\ \frac{1}{2}$, which represents the actual plane in the orthorhombic cell. To eliminate the fractions these indices must be multiplied by two, giving 321. But this multiplication of the indices by two is equivalent to halving the spacing, and thus d_{321} is only half as great as the actual spacing in the lattice.

In consequence of the above relationships, every line of the powder photograph can be given monoclinic indices hkl; most of the lines can be given directly orthorhombic indices $h'k'l'$; the remainder, when referred to the orthorhombic unit, have spacings equal to $2\times d_{h'k'l'}$. Table 2 shows this relationship for the first twelve lines of the powder photograph.

Palacios and Salvia did not attempt to assign indices to the nineteen powder photograph lines which they assumed to be orthorhombic, so no comparison can be made. The assignment of monoclinic indices would be even more difficult, were it not for the fact that completely indexed Weissenberg photographs were available. Interplanar spacings were calculated for all planes whose reflections were at least moderately strong on the Weissenberg films, and these were checked against the spacings determined from the powder photographs. In many cases there is more than one choice, and it is quite probable that the powder photograph

---

[3] This is the reverse of the convention whereby multiple indices such as 200, 300, etc., are used to indicate fractional spacings of 100; in this case fractional indices are used to indicate multiple spacings.

TABLE 2. OBSERVED SPACINGS FOR SOME OF THE LINES OF THE MONOCLINIC POWDER PHOTOGRAPH, WITH CALCULATED SPACINGS FOR THE PSEUDO-CELLS

Monoclinic		Pseudo-orthorhombic		Pseudo-cubic		
d (obs.)	hkl	$h'k'l'$	d (calcd.)	$h''k''l''$	d (calcd.)	$\frac{a_0}{d}$
3.91	200	101	3.90	211×2	3.96	
	$20\bar{2}$	$10\bar{1}$				
3.40	002	002	3.42	011	3.40	$\sqrt{2}$
	210	111	3.393	110		
	$21\bar{2}$	$11\bar{1}$		$10\bar{1}$		
3.07	012	012	3.073	031×2	3.06	
2.81	$31\bar{1}$	321×2	2.809	$63\bar{1}$×4	2.85	
2.66	121	143×2	2.65	$27\bar{1}$×4	2.63	
2.58	220	121	2.586	231×2	2.58	
	$22\bar{2}$	$12\bar{1}$				
2.44	$11\bar{3}$	$12\bar{5}$×2	2.46	$2\bar{3}\bar{7}$×4	2.46	
	$31\bar{3}$	$32\bar{3}$×2	2.43	651×4	2.46	
	022	022	2.436	020	2.42	$\sqrt{4}$
2.37	$40\bar{2}$	200	2.367	200		
2.205	$13\bar{1}$	$16\bar{1}$×2	2.21	275×4	2.19	
2.08	$12\bar{3}$	$14\bar{5}$×2	2.095	291×4	2.09	
	202	103	2.055	233×2	2.06	
2.05	$20\bar{4}$	$10\bar{3}$				
1.99	230	131	1.985	$12\bar{1}$	1.98	$\sqrt{6}$
	$23\bar{2}$	$13\bar{1}$		$11\bar{2}$		
	212	113	1.97	121		
1.96	$21\bar{4}$			$1\bar{1}\bar{2}$		
	400			211		
1.72	040			$02\bar{2}$	1.71	$\sqrt{8}$
1.54	042			$03\bar{1}$	1.53	$\sqrt{10}$
	232			130		
	024			031		
1.30	250			$13\bar{2}$	1.29	$\sqrt{14}$
	214			132		
	422			231		
	440			$23\bar{1}$		
1.23	044			040	1.21	$\sqrt{16}$
1.155	060			$03\bar{3}$	1.14	$\sqrt{18}$
	252			$14\bar{1}$		
	234			141		
	$25\bar{4}$			$11\bar{4}$		
1.09	062			$04\bar{2}$	1.08	$\sqrt{20}$
.965	800			422	.99	$\sqrt{24}$
	254			150	.95	$\sqrt{26}$
.94	216			143		

line is a composite one. A few lines had to be indexed in terms of planes whose Weissenberg reflections were rated as weak, and in a few cases alternative indices are given, corresponding to planes which could not have reflected on any of the particular photographs taken.

Palacios and Salvia conclude that both the high and the low temperature modifications are present simultaneously at room temperature, the former being in a metastable condition. They assume that the two forms occur in a mosaic, in which orthorhombic (100) is parallel to the three cube planes (100), (010) and (001). When using the Bragg spectrographic method, this should result in a split reflection from a cube face of argentite, one reflection being from cubic d_{200} and the other from orthorhombic d_{200}. They obtained a split reflection, and in further support of this hypothesis, they cite their powder photographs, supposedly consisting of both cubic and orthorhombic lines.

The writer believes that this hypothesis is entirely without foundation. If for some unexplained reason, a cubic crystal of argentite, formed above 180°C., remains partly cubic upon cooling, while a portion inverts, how could a monoclinic (pseudo-orthorhombic) crystal of acanthite, formed below 180°C., have both the high and low temperature modifications present? This would have to be the case, for argentite and acanthite give identical powder photographs.

It has already been pointed out that all of the lines of the powder photograph can be indexed as monoclinic. The indexing of some of the lines as cubic, and the occurrence of the split reflections remain to be explained. The monoclinic unit cell is not only pseudo-orthorhombic, but also pseudo-cubic. The pseudo-orthorhombic cell has values of a, b and c such that a, $b/\sqrt{2}$ and $c/\sqrt{2}$ are almost equal. This makes possible the pseudo-cube shown in Fig. 6*b*, with a_0 having an average value of about 4.82Å. Like the orthorhombic cell, this cube is only a ficticious unit, for not all of its corners are marked by lattice points, and adjacent cubes are not identical. Also, the three cubic axes are not quite at right angles to each other. But any $h''k''l''$ plane in this pseudo-cube will be an hkl plane in the monoclinic cell. Because of the vacant lattice positions in the cube, the reverse is not always true. Certain monoclinic spacings have no direct counterpart in the cubic lattice, being either two or four times as large as the cubic spacings should be. Thus not all of the powder photograph lines can be indexed directly as cubic. The transformation from monoclinic to cubic is

$$\tfrac{1}{2}00/\tfrac{1}{4}\tfrac{1}{2}\tfrac{1}{2}/\tfrac{1}{4}-\tfrac{1}{2}\tfrac{1}{2}.$$

With this formula it is possible to determine which of the monoclinic planes can be referred directly to the cubic lattice. There are twelve of these planes, as shown in Table 2. Nine of these twelve are among the lines listed by Palacios and Salvia as cubic. They missed the other three, but had four additional ones, which are incorrect. In any pattern with a large number of lines, it usually happens that certain ones will have spacings which by chance agree approximately with any choice of unit cell. The four extra lines are of this type. They were indexed as 111, 311, 331 and 333, respectively, by Palacios and Salvia. These particular cubic planes, when transformed to the true monoclinic cell, become 201, $60\bar{1}$, 621 and 603. All of these have $h+l\neq 2n$, and hence none may reflect in a B-centered lattice, and should not occur. The interplanar spacings in the cubic system are calculated by the formula $d_{hkl}=\frac{a_0}{\sqrt{h^2+k^2+l^2}}$. Thus the spacings for cubic 111, 311, 331 and 333 are respectively as follows: $\frac{a_0}{\sqrt{3}}$, $\frac{a_0}{\sqrt{11}}$, $\frac{a_0}{\sqrt{19}}$ and $\frac{a_0}{\sqrt{27}}$. These four lines, mistaken by Palacios and Salvia for cubic, are actually reflections from monoclinic $31\bar{1}$, 133, 016 and 226. When converted to the cubic lattice, their spacings are 631×4, 2·13·1×4, 075×2 and 295×2, which are equivalent to $\frac{4a_0}{\sqrt{46}}$, $\frac{4a_0}{\sqrt{174}}$, $\frac{2a_0}{\sqrt{74}}$ and $\frac{2a_0}{\sqrt{110}}$, respectively. The comparable spacings for the four planes listed by Palacios and Salvia may be written as $\frac{4a_0}{\sqrt{48}}$, $\frac{4a_0}{\sqrt{176}}$, $\frac{2a_0}{\sqrt{76}}$ and $\frac{2a_0}{\sqrt{108}}$. These are so close to the actual spacings that it is easy to see how the error was made.

From the foregoing, two conclusions may be drawn. (1) The fact that twelve lines of the powder photograph can be given cubic indices $h''k''l''$ does not imply the presence of a cubic modification, but results solely from the pseudo-cubic character of the monoclinic cell. (2) The pseudo-cubic cell cannot be based on a Cu_2O-type of structure, for the twelve reflections do not correspond to those to be expected from such a type. The four reflections, 111, 113, 133 and 333, all supposed to be present by Palacios and Salvia, are actually missing. These reflections would all be required by a Cu_2O-type structure, and would be comparatively strong.

In order to determine the significance of the split reflections reported by Palacios and Salvia, zero level Weissenberg photographs were taken about each of the three a axes of an argentite cube. The specimen was from Freiberg, Saxony, and showed well developed $\{211\}$ faces truncating the cube corners. The photographs indicate that the argentite cube consists of a mosaic, not of the high and low temperature modifications as proposed by Palacios and Salvia, but rather of monoclinic pseudo-cubes in various orientations.

The pseudo-cube in a crystal of acanthite is bounded by monoclinic $(\bar{2}01)$, (011) and $(01\bar{1})$. When an argentite crystal inverts, it would seem reasonable to assume that any one of the three cube planes might become monoclinic $(\bar{2}01)$. Since the three cube planes are identical, there should be an equal probability for each, and hence all three orientations might be expected. That is, in different portions of the inverted crystal, monoclinic $(\bar{2}01)$ may be parallel to the original cubic (100), (010) and (001). Furthermore, each of these orientations could have either of two positions, 90° apart. The identical cubic directions [011] and $[01\bar{1}]$ are parallel to the b^* and c^* directions in the monoclinic. After inversion, either of the two cubic directions may be b^* or c^*. The two possibilities represent two positions about the monoclinic a axis, 90° apart. Hence an argentite crystal at ordinary temperatures should consist of a mosaic of monoclinic pseudo-cubes in six different orientations, but with these orientations all having marked parallelism of nearly equivalent directions.

Under these conditions, any single cube face of an argentite crystal after inversion would have parallel to it both $(\bar{2}01)$ and (011) or $(01\bar{1})$ of the monoclinic. The first has a spacing of 4.76Å, the two latter 4.88Å. First order reflections are missing from both. The second order reflections correspond to spacings of 2.38Å and 2.44Å, respectively. These must be the split reflections obtained by the Bragg method from cube faces of argentite by Palacios and Salvia, and attributed by them to d_{200} from both the high and low temperature modifications. Since monoclinic $(\bar{2}01)$ is equivalent to orthorhombic (100), this assumption gave them a correct value for their orthorhombic cell dimensions.

Although not identical, the Weissenberg zero level photographs about the three a axes of an argentite cube show no distinctive differences, thus indicating that the various orientations are randomly distributed. For a given axis rotation, the Weissenberg pattern is essentially equivalent to two superimposed monoclinic Weissenberg zero level, a axis photographs, 90° apart. The monoclinic a axis is almost exactly perpendicular to $(\bar{2}01)$, and the two possible orientations with $(\bar{2}01)$ parallel to a cube face produce this effect. Monoclinic b^* and c^* are at right angles to each other, while the directions [011] and $[01\bar{1}]$ are not quite at 90°. This causes the central lattice lines parallel to [011] and $[01\bar{1}]$ to be doubled, while those parallel to b^* and c^* are single.

In addition to the Weissenberg pattern just described, due to the two orientations of the pseudo-cube parallel to the argentite cube face, there is also the effect of the remaining possible orientations of the pseudo-cube, with monoclinic (011) or (01$\bar{1}$) parallel to the argentite cube face. For these orientations the main central lattice lines are [$\bar{2}$01] and [011] or [01$\bar{1}$]. The latter two are identical with, and fall right upon similar lattice lines of the previous orientation. The [$\bar{2}$01] central lattice line falls upon [011] or [01$\bar{1}$] of the previous orientation, and the slight difference in spacing causes doubled reflections. Other reflections between the main central lattice lines are so much alike that they are indistinguishable. Certain pairs of entirely different planes have almost equal spacings and nearly symmetrical positions. The reflections arising from such planes in the various orientations cannot be distinguished with certainty, especially since the films are of mediocre quality.

The implications of this parallelism between the monoclinic pseudo-cube and the actual high temperature cubic lattice are uncertain. It would seem reasonable to conclude that there is a close relationship between the two structures. Powder photographs of Ag_2S above 180°C. taken by Emmons, Stockwell and Jones (1926) and also verified by the author, show a cubic pattern consisting of only four lines. They are 3.40Å (*ms*), 2.42 (*s*), 1.98 (*w*) and 1.71 (*m*). They correspond closely in position, but not in intensity, to the first four lines of the monoclinic pattern to which cubic indices can be directly assigned (Table 2). The four spacings are in the simple ratio of $\frac{1}{\sqrt{1}}:\frac{1}{\sqrt{2}}:\frac{1}{\sqrt{3}}:\frac{1}{\sqrt{4}}$, and by themselves may be indexed in several ways. But the indices 110, 200, 211 and 220 are the only simple ones which correspond to a unit cube containing an integral number of formula weights, providing that the density of Ag_2S at room temperature, 7.2, is assumed also to be the density of the cubic form. This unit cube has $a_0 = 4.84$Å, contains $2Ag_2S$, and corresponds directly with the monoclinic pseudo-cube. The four lines of the cubic pattern, and the twelve of the pseudo-cubic, are those characteristic of a body-centered lattice. But there are objections to such a simple solution. No cubic space groups based on a body-centered (I) lattice have special positions for four atoms. Among all of the cubic space groups there are only five which provide special positions accommodating both 2 and 4 atoms, and because of duplication, these five actually represent only two different structure types. In both, the two S atoms would be at 000 and $\frac{1}{2}\frac{1}{2}\frac{1}{2}$, while the four Ag atoms would have either positive or negative tetrahedral arrangements at $\frac{1}{4}\frac{1}{4}\frac{1}{4}$, etc., or xxx, etc. The former represents the Cu_2O-type; the latter would not be expected unless the two atoms at 000 and $\frac{1}{2}\frac{1}{2}\frac{1}{2}$ were different in size. The light S atoms at the positions 000 and $\frac{1}{2}\frac{1}{2}\frac{1}{2}$ would not be able to influence sufficiently the diffraction effects to give a body-centered pattern. There is no way in which a tetrahedral arrangement of four Ag atoms could even remotely simulate a body-centered structure.

Because of the wrong assignment of indices to their pseudo-cubic pattern, Palacios and Salvia thought they had proof of a Cu_2O-type of structure. This would require a Ag-S distance of about 2.10Å. The exact type of bonding in Ag_2S is not known; it might be expected to be intermediate between the metallic and electron-pair bond types. The interatomic distance of 2.10Å is very small for either type, and would require such a high degree of polarization that it seems improbable. Moreover, as already stated, a Cu_2O-type of structure would require strong reflections from planes such as 111, 113, etc., which are not found on photographs taken above 180°C.

Two possible solutions of this dilemma might be mentioned. The fact that the pseudo-cube is a ficticious unit, with only part of the lattice corners occupied, and with adjacent cubes different, suggests that the true cubic unit might be a multiple of this pseudo-cube, with $a_0 = n \times 4.84$Å. This larger unit could then legitimately have missing atoms at the corners of some of the sub-cubes, and the possible positions for the $n^3 \times 4$ Ag atoms would be greatly increased. However, when a complex structure gives diffraction effects simulating those of a simple structure, it usually means that it actually deviates only slightly from such a simple structure. On the average, there would still have to be four Ag atoms in each sub-cube, and although no longer restricted to a tetrahedral arrangement, the possibility of simulating a body-centered structure seems remote. The second possible solution would be a defect lattice, in which the Ag atoms were distributed at random over only a portion of the positions normally required by cubic symmetry. Conjectures concerning these and other possibilities might better be left until Weissenberg data from argentite crystals above 180°C. are available.

No light is thrown on the cubic structure of Ag_2S by the chemically similar compound Cu_2Se. This compound is cubic, and was reported by Davey (1923) to have a CaF_2-type of structure. The author has checked this by means of both powder and Weissenberg photographs of octahedral crystals of Cu_2Se, obtained by passing Se vapor over hot Cu. Cubic Ag_2S and cubic Cu_2Se are not isomorphous.

Morphology of Acanthite

The very close approximation of the true monoclinic unit cell to an orthorhombic unit is sufficient to account for the previous classification of acanthite as orthorhombic. Pairs of planes, such as (100) and $(10\bar{1})$, (101) and $(10\bar{2})$, etc., are so nearly symmetrical in position that their measured angles would be practically indistinguishable, especially when the poor quality of the usual goniometric measurement on acanthite is considered. This pseudo-symmetry is very apparent in a gnomonic projection constructed normal to the *a* axis (Fig. 7). In such a projection the center is almost exactly halfway between the face poles for (100) and $(10\bar{1})$.

Added to this pseudo-symmetry is the mimetic effect of the polysynthetic (001) twinning. Thus on type 1 crystals, the main terminal face is not $(10\bar{1})$ but a combination of (100) from one twin orientation and $(10\bar{1})$ of the other. A similar situation prevails for all other terminal faces. It might be expected that when there is a distinct monoclinic character, as in the type 1 crystals, or in that described by Groth from Annaberg, the crystal would consist chiefly of one of the two twin orientations. If the two orientations are present in nearly equal proportions, orthorhombic symmetry would be simulated. Even in the former case, however, the measured angles could be interpreted as orthorhombic.

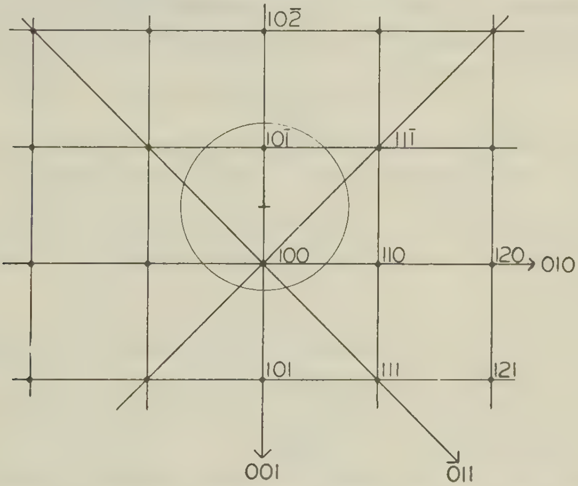

FIG. 7. Gnomonic projection perpendicular to the *a* axis. The points do not represent observed faces, but merely internal planes. Poles 100 and 101 are nearly equi-distant from the projection center, resulting in a pronounced pseudo-symmetry. Because of the near equivalence of *b* (6.92Å) and *c* sin *β* (6.86Å) the projection appears tetragonal.

The possible interpretation of acanthite as cubic was pointed out by Krenner (1888), who concluded that acanthite actually is cubic. In a personal communication, Professor Charles Palache told the author that he had never measured a crystal of acanthite that could not be interpreted as cubic. The explanation of this of course lies in the fact that the monoclinic lattice is not only pseudo-orthorhombic, but also pseudocubic. In this connection it should be pointed out that although in some cases the monoclinic *spacings* d_{hkl} have no direct counterpart in the two pseudo-cells (Table 2), every monoclinic *plane hkl* is parallel to a corresponding plane $h'k'l'$ and $h''k''l''$ in the pseudo-cells. As a result, every monoclinic face can also be given both orthorhombic and cubic indices. Krenner gives a table of corresponding angles and indices for the cubic and orthorhombic interpretations, and this is exactly what would be expected from the two pseudo-cells. The measured range of angles between any pair of faces almost invariably extends on both sides of the value to be expected from a cubic crystal.

As can be seen readily from the gnomonic projection in Fig. 7, as well as from the orthorhombic axial ratio $a:b:c=0.6886:1:0.9944$, the structure also possesses a pronounced pseudo-tetragonal character. But so far as the author is aware, no one has considered the true symmetry of acanthite to be tetragonal.

Summary

The data obtained from the Weissenberg and powder photographs of Ag_2S at room temperature may be summarized as follows:

Acanthite, Ag_2S
$a=9.47$ Å
$b=6.92$
$c=8.28$
$c \sin\beta=6.86$
$\beta=124°$
Cell volume $=449.8$ Å^3
Cell contents $=8$ Ag_2S
$d_{(\text{lit.})}=7.22$
$d_{(\text{calc.})}=7.27$

Monoclinic; $a:b:c=1.368:1:1.96$ (x-ray).
Probable space group $B2_1/c$ (C_{2h}^5).

hkl absent when $h+l$ is odd.
$h0l$ absent when either h or l is odd.
$0k0$ absent when k is odd.
Polysynthetic twinning (001) observed on all crystals.
Contact twinning (100) on type 2 crystals only.

The previous assignment of acanthite to the orthorhombic and cubic systems on the basis of morphology, and the interpretation of the x-ray data as indicating orthorhombic and cubic lattices, are both explained by the pseudo-orthorhombic and pseudo-cubic character of the actual monoclinic cell. The close correspondence of the interfacial angles with those of systems with higher symmetry is due to the cell dimensions. The occurrence of crystals with apparent orthorhombic symmetry is due both to cell dimensions and to the mimetic effect of the polysynthetic twinning.

It seems probable that the high-temperature cubic lattice is closely related to the pseudo-cubic cell, and that neither is based on a Cu_2O-type of structure. It is not isomorphous with cubic Cu_2Se. No other conclusions are drawn as to the structure of the cubic form, either with respect to dimensions or atomic positions.

ACKNOWLEDGMENT

The author wishes to thank the Executive Board of the Horace H. Rackham School of Graduate Studies for a grant from the Faculty Research Fund which made possible the purchase of some of the equipment used in this investigation.

REFERENCES

DAUBER, *Ber. Ak. Wien.*, **39**, 685 (1857).

DAVEY, W. P., *Phys. Rev.*, **21**, 380 (1923).

EMMONS, R. C., STOCKWELL, C. H., AND JONES, R. B. H., *Am. Mineral.*, **11**, 326 (1926).

GROTH, P., *Min. Samml.*, **57** (1878).

HARCOURT, G. A., *Am. Mineral.*, **27**, 71 (1942).

KRENNER, J., *Zeits. Krist.*, **14**, 388 (1888).

PALACIOS, J., AND SALVIA, R., *Anal. Españ. Fis. y Quim.*, **29**, 269–279 (1931); abstract in *Strukturbericht* **II**, 283.

RAMSDELL, L. S., *Am. Mineral.*, **10**, 286 (1925); **12**, 25 (1927).

ALKALINE VITROPHYRE DIKE, CAPE NEDDICK, MAINE

John C. Haff, *Colorado School of Mines, Golden, Colorado.*

Abstract

In this paper is presented a detailed petrographic description of an unusual alkaline vitrophyre dike intruding a mass of breccia on Nubble Island, off Cape Neddick, Maine. The rock possesses strong flow banding, skeletal crystals, several varieties of incipient spherulitic structures, and contains devitrification aggregates typical of modified pitchstones. Chemical analysis indicates its strong nordmarkitic or sölvsbergitic affinities, suggesting its relationship to the paisanitic and monchiquitic dikes which cut riebeckite granite at nearby York Beach.

Introduction

The narrow peninsula of Cape Neddick lies one-half mile southeast of York Village, Maine, and extends eastward from the coastline for about one and one-quarter miles. Separated from this peninsula by a narrow gut is a small, elongate, rocky island. Though not named on either U. S. Coast and Geodetic Survey chart (No. 228, Cape Neddick Harbor to York River) or U. S. Geological Survey map (York quadrangle, Maine-New Hampshire), this island is locally called the "Nubble." On it stand the Cape Neddick lighthouse and a few small outbuildings. The major axis of the island, which is over 800 feet long, strikes about N. 10°E. Its eastern side is penetrated by two coves, between which crops out the distinctive glassy dike that is described in this paper.

Local Geologic Relations

The central and western parts of the island are underlain by massive, coarse-textured, hornblende gabbro (Wandke, 1922, p. 151). Near the western side a pegmatitic facies of the gabbro is exposed the entire length of the outcrop (Fig. 1). The gabbro intrudes the Carboniferous (?) Kittery quartzite (Katz, F. J., 1918, p. 168), which latter rock is cut by many diabasic dikes. The quartzite crops out only in the southeastern part of the island and consists of alternating thin ($\frac{1}{4}''$–$\frac{1}{2}''$) purplish, micaceous laminae and thicker (2′–4′) massive, light gray, quartzose beds. Between the quartzite and gabbro, and extending the entire length of the island, is a mass of structurally and lithologically complex breccia. This consists predominantly of quartzite and basic dike-rock fragments set in a dense, fine-textured and well indurated matrix (Haff, 1939, p. 470).

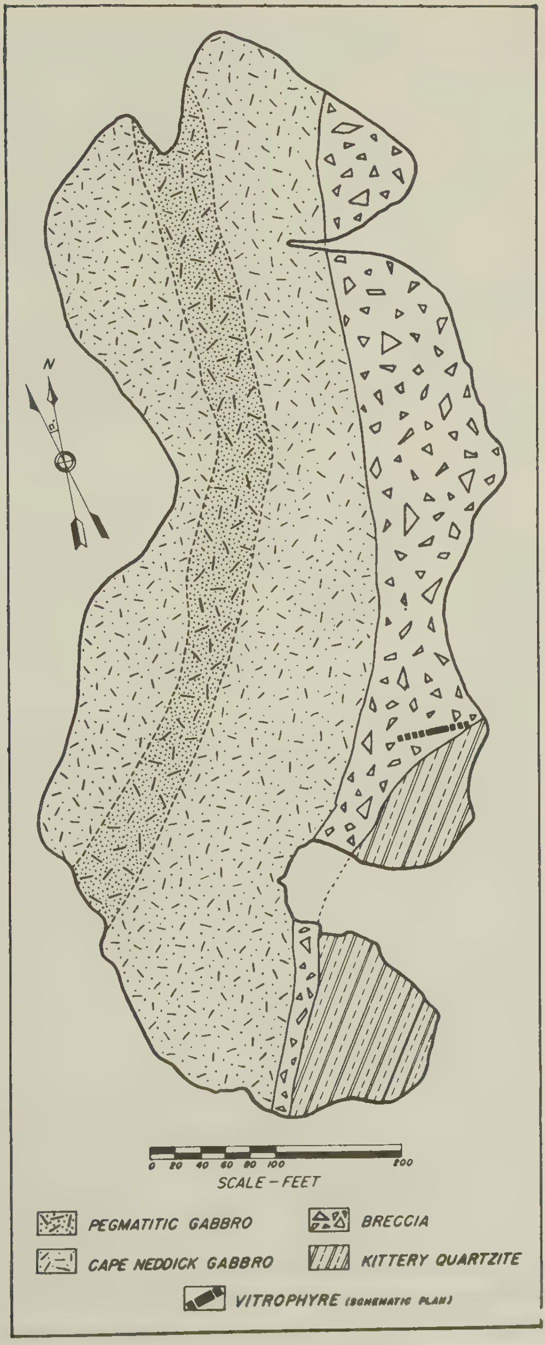

FIG. 1. Geologic sketch map of Nubble Island, off Cape Neddick, Me., showing the areal distribution of major rock types and location of vitrophyre dike.

Between the two coves on the eastern side of the island the breccia is intruded by a narrow dike which ranges in strike from approximately west to N.60°W. in its small exposure. This dike varies from 5–8 inches in thickness, thins rapidly and possesses the dimensions given for only a few feet along the outcrop. The mass cannot be traced with certainty into either gabbro or quartzite. Definite evidence of chill against the breccia can be observed in the field. Its intrusive relation is further substantiated by the presence of conspicuous flow lines near its contacts, and of small glassy apophyses penetrating the breccia.

On the weathered surface the dike varies from a dark olive-green color to buff. White, or yellowish, tabular feldspar phenocrysts and conspicuous flow lines parallel to contacts are the only structures visible megascopically. On the fresh fracture the rock is dense, greenish-black in color, and possesses a dull, but in places slightly resinous, lustre and conchoidal fracture.

Microscopic Petrography

Microscopically this rock is conspicuously porphyritic. Fluxion structure is also prominent throughout although especially so in the chilled marginal portions.

The rock consists for the most part of haphazardly mottled, turbid, brown glass, bearing numerous crystallites and occasional relatively large euhedral plagioclase and hornblende phenocrysts. The delicate and minute, transparent, slightly greenish crystallites are usually acicular in form. They often taper or bifurcate at their extremities, are feebly birefringent, and have parallel extinction. Unmodified glass from the dike margins has an average specific gravity of 2.588 and an index of refraction of 1.535 ± .002. Accessory apatite occurs sparingly in minute, slender prisms and small grains of magnetite, chlorite and yellowish-green epidote are scattered throughout the groundmass. The fine, granular epidote is often associated with minor amounts of carbonate. Here and there are subhedral pyrite grains averaging 0.5 mm. across, which have in places replaced magnetite.

The brown glass is modified to varying degrees in irregular fashion. Where still wholly vitreous, as in the chilled marginal phases of the dike, it is light brown or a pale café-au-lait color. The glass in the interior of the dike is usually appreciably altered. It is extremely turbid in aspect, has a dark, greenish-brown color, in places is very feebly birefringent as the result of the presence of cryptocrystalline devitrification products, and is nearly opaque in a thin slice. Throughout the rock there is sharp color contrast, in shades of brown and greenish-brown, between flow bands. Adjacent bands nearly always show slightly different internal structure and exhibit different degrees of modification, probably as the result of slight variations in original composition.

Near the dike margins some parts of the pale brown, glassy chill-zone show feeble anisotropic effects. These do not result from the development of devitrification aggregates but occur in streaks whose distribution is related to that of the flow bands. It seems most probable that the anomalous anisotropism in the dike selvages is caused by strain resulting from deformation subsequent to intrusion.

The turbidity of the glass in the greater part of the rock results from the presence of both secondary substances and exceedingly fine crystalline devitrification products developed at the expense of the glass. However, no individualized mineral grains sufficiently well developed to be susceptible of positive identification could be detected. At best only irregularly dispersed, microscopically irresolvable, mote-like specks and dirty brown aggregates can be seen. En masse these substances have a somewhat higher refringence than the surrounding glass and are darker brown than the unmodified portions of the mesostasis. The confused optical data obtained from these fine, disseminated products suggest that they probably consist of intimately mixed epidote and turbid carbonate. In places, small, clear, colorless areas consisting of albitic feldspar and carbonate occur in the ground-mass. In some parts of the rock several such albitized patches may show uniform optical orientation over short distances.

The few hornblende phenocrysts present vary from 0.5–2.0 mm. in length, show excellent cleavage and are of prismatic habit. Unmodified crystals have $2V_\alpha = 86° \pm 2°$, show strong pleochroism, X, dark greenish-brown; Y, deep brown; Z, light yellow-brown; $X > Y > Z$, and have a maximum extinction angle $Z \wedge c$ of 15°–18°. Most of the hornblende originally present is represented by fibrous aggregate pseudomorphs of yellowish-green, actinolitic amphibole intergrown with magnetite, leucoxene, chlorite, and minor amounts of carbonate. There has been conspicuous selective alteration of the hornblende. In some of the dense, structurally homogeneous bands of glass it is quite fresh; in many with spherulitic structure it has been wholly replaced by granular magnetite. In pseudomorphs of this latter type the magnetite grains are often oriented along pre-existing cleavages.

A type of pseudomorph different from those after hornblende also occurs. Relicts of this second variety usually show definitely square or rectangular cross-sections, and consist of matted, fibrous amphibole, carbonate, chlorite, epidote, pyrite, magnetite and apatite euhedra. They differ essentially from those obviously after hornblende in that carbonate and apatite are everywhere much more abundant in them.

Former pyroxene, rather than olivine, is suggested by these aggregates.

The oligoclase-andesine phenocrysts (Ab_{67}–Ab_{70}) are uniformly dispersed throughout the rock but in places may show cumulophyric arrangement. When thus disposed as many as 10 to 12 sharply euhedral crystals, from 0.5–2.5 mm. in length, frequently comprise an assemblage. The plagioclase is water-clear, or at most only slightly sericitized. The phenocrysts are polysynthetically twinned on the albite, pericline and combined Carlsbad-albite laws. Zoning is usually inconspicuous and evidences of marginal resorption are rare. The larger plagioclase phenocrysts show conspicuous pinacoidal development. The smaller ones tend to be more irregular in outline and, though in part tabular, often bear narrow, wedge-shaped, tapering processes extending from the corners of the crystals. Some of the incipient phenocrysts exhibit triangular cross-sections and in these the steeply pitching boundary surfaces may be seen through the translucent glass below the thin-section surface. This produces the effect of a broad, poorly defined phantom margin merging with the groundmass rather than a sharply defined contact.

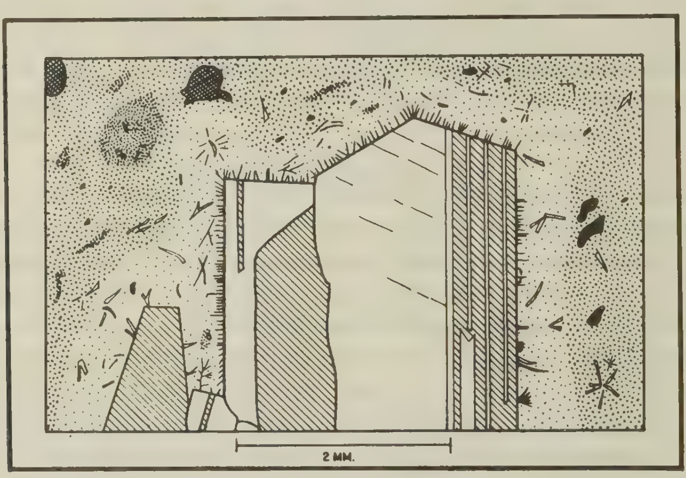

Fig. 2. Camera lucida drawing of a clarified glass zone around a plagioclase phenocryst and the characteristic fringing microlites attached to its margins. Turbid glass of groundmass is heavily stippled; cross-hatched areas are hornblende grains.

Attached to the margins of many plagioclase phenocrysts are delicate, transparent or slightly greenish crystallites (longulites). These have grown as individuals or as clusters of minute prisms radiating from points on the crystal margin. Individual crystallites tend to be nearly uniform in length on a given crystal, stand perpendicular to the crystal margins, and form conspicuous comb-like fringes (Fig. 2). So far as can be determined the crystallites attached to plagioclase are identical with those scattered elsewhere throughout the glass. The formation of these fringing crystallites has caused the glass immediately surrounding the phenocrysts to be depleted of certain substances (cf. Tyrrell 1928, p. 225–226). Hence around each phenocryst bearing such a fringe is a narrow zone of glass of lighter color than that found elsewhere in the rock. Further, these lighter zones are relatively free from the granular alteration products often so abundant in the glass. The outer limits of the clarified areas are demarcated by narrow, quasi-continuous zones congested with dark-colored secondary products. At the corners of the fringed plagioclase crystals the light-colored zone widens and protrudes beyond its general limits roughly parallel to the enclosed phenocryst.

Opaque, dark brown to black, skeletal crystal growths, which may approach in overall dimensions the larger phenocrysts, occur in the glass, usually in or near the chilled selvages. These growths consist of magnetite, rutile (?), and leucoxene with some associated epidote. They have no definite boundaries (Pl. I C). In them, thin plates, rods and granules of opaque minerals are arranged in uniformly spaced parallel rows which are variable in length within a single skeletal unit. Transverse, rod-like members usually connect the long parallel rows and thereby form a reticulate network. The parallel rows in an individual skeletal growth have no common orientation with respect to nearby growths, nor is their disposition related to flow structures. These skeletal structures sometimes indiscriminately traverse spherulitic structures in the rock and one network may embrace several of the latter. No semblance of suggestive crystal form or cleavage could be detected in them, although such structures may possibly represent incipient pyroxene.

All the phenocrysts are definitely intratelluric. The flow lines in the glass uninterruptedly swirl around and arch over both individual phenocrysts and glomeroporphyritic aggregates. The plagioclase phenocrysts are consistently oriented with their long axes closely conformable in direction with that of the local fluxion structure. Many plagioclase phenocrysts in the chilled selvages have been much fractured and in some cumulophyric groups the crystals have been reduced to a jumble of shattered and irregularly oriented fragments (Pl. I D). Such structures might conceivably result either from relief of stresses upon cooling, or from post-consolidation movements. In either case the surrounding glass itself should likewise show some evidences of strain. However, the glass enclosing these shattered crystals is not fractured and continuous flow lines pass around the fractured crystals and aggregates. It seems more likely that these phenocrysts were broken by flowage of the viscous magma during its intrusion rather than by any later mechanical dislocation of the solidified glass.

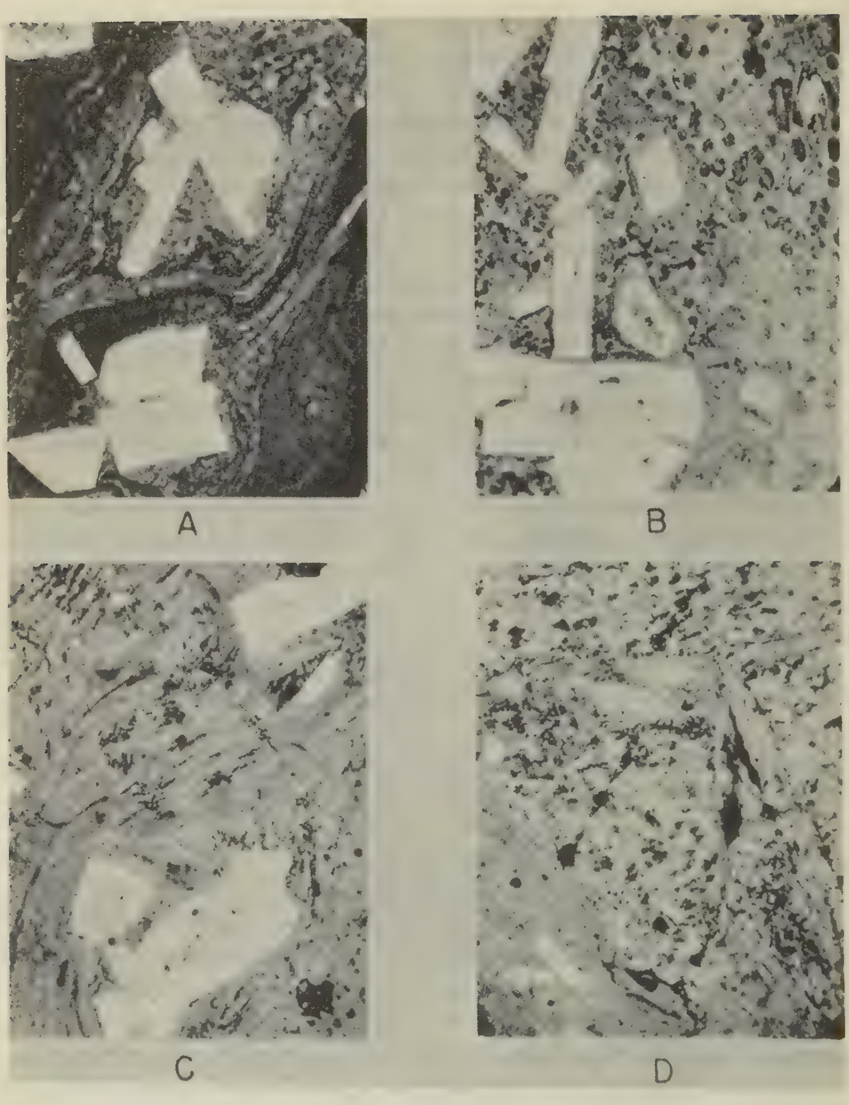

Plate I

A. Photomicrograph taken to show the strong flow structure in the glass and the cumulophyric arrangement of plagioclase phenocrysts. The variability in color and microstructure in the different flow bands and the tendency for incipient spherulitic structures to be developed in the clearer glassy portions are quite evident. Mag. 13×, plane polarized light.

B. Photomicrograph showing the clarified rims developed about the euhedral plagioclase phenocrysts and the rudimentary spherulitic structures which are dispersed throughout the lighter-colored portions of the glass. Mag. 18×, plane polarized light.

Fluxion Structures

A most conspicuous feature of this rock is its fluxion structure. Under the microscope individual flow bands in the glass, which are usually from 0.8–1.00 mm. wide, are manifestly variable in both composition and internal structure (Pl. I A). Some are crowded with stellate crystallite aggregates and incipient spherulites. The latter are especially abundant in the glassy marginal phases of the dike although they occur generally throughout the entire rock. Almost the entire area of some flow bands is so densely crowded with spherical growths of circular cross section that the groundmass glass is virtually excluded. In such instances polygonal cross-sections through the rudimentary spherulites are often encountered because of the mutual interference of the contiguous spheroids. The thin and attenuated flow lines, such as are evident in spherulitic bands because of parallel alignment of crystallites and streaked coloration effects, are not diverted by the spherulitic growths. Often the fluxion lines terminate abruptly against the boundaries of the spherulites; a relationship indicating that the formation of some of these followed intrusion. Where the spherulites occur in flow bands which have been deflected around phenocrysts, the former also appear to have developed *in situ*. The termination against spherulitic structures of subsidiary streaks and lines within the curved flow band itself substantiates this.

There is much variation in size and mode of distribution of spherulites within a single flow band. They may be randomly dispersed, strung out singly in rows, or several in contact may form bead-like assemblages. Spherulitic bands are not sharply demarcated from contiguous bands exhibiting different structure but often merge into them horizontally. Spherulitic zones near the dike margins are extremely vitreous, have a high content of relatively unmodified glass, and extend to the actual contacts. It is in such zones that the glass interstitial to the spherulites has the anomalous doubly refractive character to which allusion has been made.

Other bands consisting of dense, brownish, structurally homogeneous glass contain mere traces of streaked fluidal structures internally. Except for sporadic phenocrysts such bands are quite uniform despite the presence of irregularly distributed, turbid patches through which may be scattered a few crystallites.

C. Photomicrograph showing the skeletal crystals consisting of black, opaque rods and plates in parallel arrangement. The orientation of these skeletal units shows complete disregard for flow structures in the glass. Mag. 13×, plane polarized light.

D. Photomicrograph of a minute glass apophysis penetrating a fragment of quartzite in the enclosing breccia. The greenish-brown glass contains a few shattered plagioclase phenocrysts, prominent flow structures and several incipient spherulites with conspicuous nuclei. Mag. 18×, plane polarized light.

Bands containing swarms of minute, pale-green, oriented crystallites (longulites) set in brown glass also occur. The longulites, although showing minor variations in direction within a given band, rarely depart much from parallelism with respect to its general direction. Bands carrying crystallites in abundance are lighter in color and less turbid than some others because of a relative lack of alteration aggregates in the vitreous matrix. It is in bands such as these that the greenish crystallites fringing the plagioclase phenocrysts are especially conspicuous.

Irrespective of their different structural characteristics none of the flow bands is continuous for appreciable distances. The boundaries between contiguous bands of contrasting structure usually remain parallel for a few centimeters and then converge; thus the bands pass laterally into others with different internal structures. However, the spherulitic zones in the chilled selvages are much more persistent and apparently continuous along the entire outcrop of the dike.

Incipient Spherulitic Structures

The spherulitic growths in the rock range from 0.2–0.5 mm. in diameter and nearly all of them are definitely rudimentary as regards perfection of internal structure. The majority have almost perfectly circular outlines but a few are oval or elliptical in cross section. Where several have coalesced more complex lobate outlines are presented. Though the spherulites within a given flow band may be approximately uniform in dimensions, there is considerable size variation between those in different bands.

Several growth stages in the development of these incipient spherulites or orbicules can be observed. Primitive ones, invariably small, simply consist of one or more narrow, concentric rings (shells) of dark, finely granular material enclosing lighter colored areas of glass. At the center of these circular areas there is usually a nucleus of material exactly like that forming the periphery. The nuclei may be mere pin-points or may occupy as much as one-third of the total cross-sectional area. The substances forming both the dark annulae and the nuclei do not differ in appearance from the secondary aggregates found elsewhere throughout the rock (Pl. I B).

In these rudimentary structures the lighter colored parts between the nucleus and the outer ring or rings are sometimes feebly polarizing. In certain flow bands the material in the outer ring of these spheroidal growths has been replaced by vermicular chlorite. In some parts of the glass even more simple, merely spherical aggregates were developed, but have been replaced by epidote and carbonate.

Somewhat maturer structures, approaching more closely the true spherulitic forms, have a glassy center at which microlites have developed. In these structures both the dark nuclei and concentric rings are absent. The microlites in the more abundant of these radiate directly from a center which is coincident with that of the spherulite itself. In others microlites radiate from several centers all eccentric with respect to the structure as a whole. Where several stout radiating microlites occur within the growth, a typical axial cross may be readily apparent under crossed nicols with high illumination. In places large microlites are arranged in the form of a simple cross from whose limbs smaller microlites have grown perpendicularly. Spherulitic structures of oval or elliptical cross section often contain a single large microlite, whose long axis lies parallel to the elongation of the oval, to which are attached smaller microlites set normal to its long axis.

Where the spherulitic forms are dispersed in narrow bands consisting of a single row of spheroids, the adjacent glass matrix has a sharply scalloped configuration. In bands congested with these structures the interstitial glass is clearer than that in adjacent areas and identical with that surrounding the feldspar phenocrysts bearing fringes of microlites. The incipient spherulitic structures which contain no nuclei are most abundant in the chilled margins of the dike and are often developed in the delicate apophyses of glass penetrating the breccia. These spherulites carry no microlites and in this respect differ from those in the interior parts of the dike which underwent a longer cooling period.

Chemical Composition of the Dike

As regards chemical composition, this glassy rock is apparently closely allied to nordmarkite and perhaps even more so to some of the hypabyssal derivatives of such magmas. It contains however somewhat less combined alkalies and slightly more ferrous iron than typical nordmarkite, nordmarkite-porphyry or sölvsbergite (Table 1). Except as regards its appreciably lower CaO content it is chemically very similar to windsorite. As in windsorite the greater part of the calcium in this dike magma has evidently been expended in the formation of oligoclase-andesine.

It may be inferred from the norm that appreciable quartz and orthoclase have both remained occult in the mesostasis, although a small amount of the potassium can probably be accounted for by the rudimentary spherulitic growths. In view of its structure and mineralogy this rock is considered to be a partially devitrified, spherulitic pitchstone or vitrophyre of rather unusual alkaline affinities. In this connection it is interesting to note the presence of other conspicuously alkaline rocks, to which this vitrophyre is probably genetically related, in the vicinity of Cape Neddick. At York Beach, less than one mile west of the occurrence herein described, there crops out a riebeckite granite stock cut by several diaschistic dikes of paisanite and monchiquite.

TABLE 1

	A	B	C	D
SiO_2	64.98	64.76	66.86	64.62
TiO_2	.46	.70	.21	.81
Al_2O_3	17.61	17.13	16.34	16.46
Fe_2O_3	1.82	1.87	2.24	1.82
FeO	2.53	1.25	1.99	2.14
MnO	trace	.19	trace	.12
MgO	.69	.33	.22	1.10
CaO	.90	1.48	.92	2.39
Na_2O	5.26	5.80	6.01	4.57
K_2O	4.53	5.70	4.07	5.21
H_2O+	.94	.20	.41	.39
$H_2O(-)$		.21	.18	.13
P_2O_5	.16	.11	trace	.21
CO_2				.11
FeS_2				.19
CuO				trace
BaO	.02	.09		.03
SrO	none			trace
ZrO_2		.11		.03
Cl		.02		.05
SO_3	.04		none	
S		.06		
Sum	99.94	100.01	99.59	100.38

Normative Minerals of rock A	
Q	13.44
or	26.69
ab	44.54
an	3.61
C	2.75
hy	4.08
mt	2.55
il	.91
ap	.34
I″.4(5) .1″.3(4)	

Niggli values Analysis A	
si	274.0
ti	1.5
p	0.3
al	43.7
fm	18.7
c	4.0
alk	33.6
k	.36
mg	.23
nordmarkitisch	

Mode of Rock A (Vol. %)	
Glass	93.00
Hornblende	2.00
Plagioclase	4.00
Rest	.20
	99.20

A. *Alkaline Vitrophyre*, Nubble Island, Cape Neddick, Maine. F. A. Gonyer, analyst, 1942.

B. *Nordmarkite*, Tonsenås, Aker, Nordmark, Norway. A. Rödland, analyst. Brögger, W. C., Die Eruptivgesteine des Oslogebietes, VII. Die chemische Zusammensetzung der Eruptivgesteine des Oslogebietes: *Skr. Vidensk.-Selsk. Kristiania* M.-N. Kl. No. 1, p. 87 (**1933**).

C. *Sölvsbergite*, Brock's Monument, Macedon, Victoria. A. G. Hall, analyst. Skeats and Summers: *Bull. Geol. Surv. Victoria*, **24**, p. 22 (1912).

D. *Windsorite*, Little Ascutney Mountain, Vermont. W. F. Hillebrand, analyst. Daly, R. A., The geology of Ascutney Mountain, Vermont; *U. S. Geol. Surv., Bull.* **209**, 47 (1903).

REFERENCES

HAFF, J. C., Multiple Dikes of Cape Neddick: *Bull. Geol. Soc. Am.*, **50**, 465–514 (1939).

KATZ, F. J., Stratigraphy in southwestern Maine and southeastern New Hampshire: *U. S. Geol. Survey, Prof. Paper* **108**, pt. 1, 165–177 (1918).

TYRRELL, G. W., Geology of Arran: *Memoir of the Geological Survey of Scotland*, 292 pp. (**1928**).

WANDKE, A., Intrusive rocks of the Portsmouth Basin, Maine and New Hampshire: *Am. Jour. Sci.*, 5th ser., **4**, 139–158 (1922).

ON THE GENESIS OF GRANITIC PEGMATITES

N. M. Uspensky, *Leningrad Institute of Mines, U.S.S.R.*

Abstract

A pegmatite vein is described in this article as representing a typical example of a large number of similar veins of the Transbaikal region. The structural peculiarities of this vein contribute information concerning the pneumatolytic-hydrothermal genesis of the pegmatite and indicate certain conditions pertaining to the genesis of pegmatites in general. Based upon this conception an attempt has been made to explain certain petrological phenomena. Especial attention has been given to the origin of graphic granite.

The pegmatites under consideration occur in Gold Mountain, Borshov range, 120 kilometers to the South of Nerchinsk Transbaikal, U.S.S.R. In 1934 the writer served as superintendent in the prospecting for piezo-quartz and monazite in this region. More than fifteen veins were discovered and these furnish the material for this article. The striking similarity in mineralogical composition, texture, and structure of all these veins makes it possible to select one of them as an example. The vein chosen shows a visible deficiency of mineralization and this feature permits the investigation of pegmatites in their embryonic stage.

Description

The mineral composition of these pegmatites is very simple. The essential components are a potash feldspar with a small amount of albite. There are also minor amounts of brown mica, monazite, magnetite, beryl, and topaz.

The structure of the vein shows bilateral symmetry (see Fig. 1), a feature common to all the veins. The bilateral plane is indicated by a row of cavities. Greatly elongated and flattened openings alternate with smaller ones of a lenticular character. The cavities are lined with druses of morion and orthoclase with a small amount of cleavelandite. There occur also the above mentioned accessory minerals. Druse-forming crystals have their roots in the adjoining zone which is a coarse-grained aggregate of quartz and feldspar. Because this aggregate has a quasi-graphic texture it is termed "pegmatoid" in this paper. The pegmatoid zone is composed of grains of quartz and feldspar which in cavities have developed into well-faceted crystals. This phenomenon is widely found in pegmatites and was also noted by the writer in other pegmatites of the Ural and Transbaikal regions. The width of pegmatoid zone is from 30–40 cm. The average grain size of the feldspar is 15–20 cm. across, and that of quartz 3–5 cm.

Adjoining the pegmatoid zone is a zone representing an aggregate having the same mineral composition, but showing a true graphic texture. There is no sharp division line between these zones that would denote an interval in the time of their formation. Moreover, individual grains of feldspar and quartz, located on the border of these zones, belong to both. It may be clearly seen that the more or less equi-dimensional quartz grains of the pegmatoid zone grow at the periphery into the elongated rods and form graphic intergrowths with the feldspar. This phenomenon is much better observed on the feldspar crystals, due to their perfect cleavage. It is clearly seen that while one half of a feldspar grain is in a quasi-graphic intergrowth with quartz, the other half is in true graphic relationship. The average thickness of the graphic intergrowth zone is from 20–25 cm., and the thickness of the feldspar grains varies from 15 to 20 cm. The length of the rods is about 15–20 cm., and their thickness varies from nearly invisible filaments to 2–3 mm.

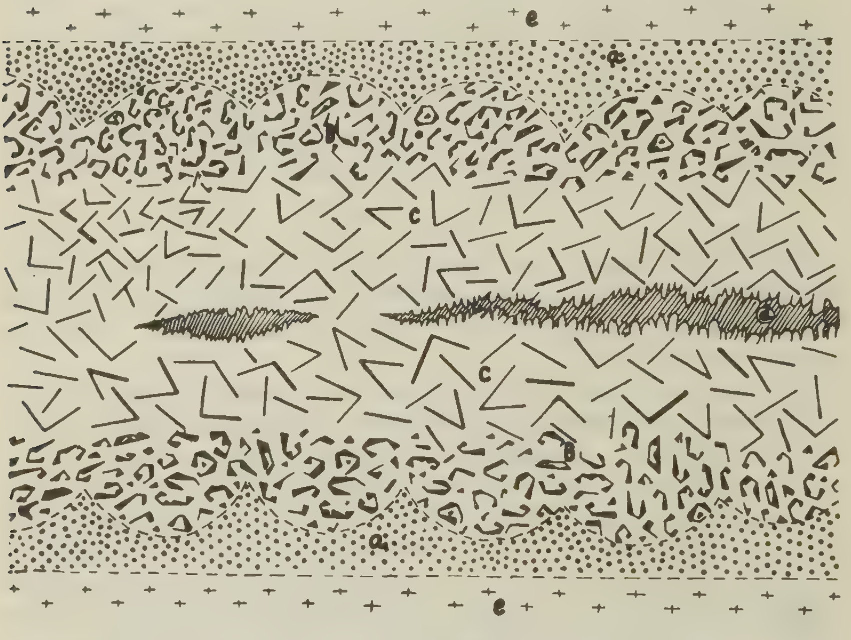

Fig. 1. a—aplite; B—graphic granite; c—pegmatoid; d—cavities; e—granite. Scale 1:14.

The graphic zone is then succeeded by common aplite. The contact between these zones is quite sharp, appearing almost as if "fused" together. There are neither cavities nor abnormal features in the boundary contacts. The aplite consists of quartz, microcline, and albite with some white and brown mica. The grains are about 1 mm. in diameter. The texture is aplitic. The contact of the aplite with the enclosing granite is sharp but there are no fractures discernible.

The granite is composed of quartz, microcline, and albite with some accessory apatite and ore minerals.

Close to the pegmatite veins considerable brown mica is disseminated in the granite. The type of contact surface between the graphic aggregate and the aplite is of a special interest (see Fig. 1). It is formed by a combination of perfectly outlined spherical segments intersecting each other. In cross-section they appear as festoons with a 10–15 cm. radius. The convex surfaces of the arcs penetrate the aplite.

However, the graphic texture itself is of much more interest (see Fig. 2). The zone of the graphic texture aggregate is made up of a series of more or less thick spherical zones. The radial character of the sections of these zones shows clearly that they in turn have a concentric zonal structure and are made up of a series of sub-zones. The sub-zone boundaries are well defined in a unique manner. The quartz rods radiate from the center of the zone. The thickness of the rods changes suddenly and simultaneously in the whole series of rods forming this intergrowth zone.

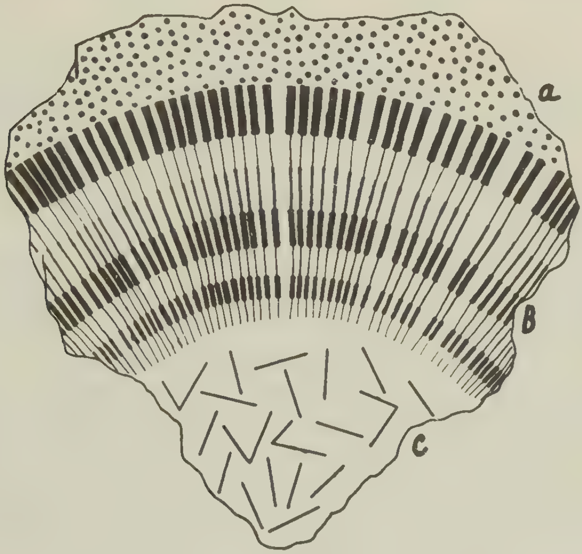

FIG. 2. Structure of the graphic granite: a—aplite; B—graphic granite; c—pegmatoid.

The rows of rods of the same thickness, which vary in different sections, seem to form sub-zones, and the ends of the sections give the impression of being the boundary lines of these sub-zones. As a whole this resembles the botryoidal structure of malachite or hematite. However this impression is not correct for the sub-zone boundaries are defined neither by fractures nor by abnormal features and are in fact only a function of the shape of these rods. The feldspar surrounding this series of rods may be a single crystal, a twin, or an irregular intergrowth of two or three crystals. The feldspar has no constant orientation in relation to the zone itself, in contrast to the quartz rods that are all oriented along the radii of the limiting segment. All these features can be observed on the feldspar cleavage planes.

These graphic intergrowths of quartz and feldspar appear in tangential cross-section like common graphic granite. In the graphic zone one may observe as many as 15 sub-zones, their thickness varying from 5–15 mm.

INTERPRETATION

I. Campbell (1) has indicated that the shape of cavities in rocks which is characterized by an alternation of pinchings and swellings with resulting wedging-out and subsequent reappearance, is the result of the activity of circulating solutions. These solutions may dissolve minerals and then deposit the dissolved material in the same cavities in the form of grain-aggregates and druses.

Evidently, a similar process took place in veins at the time of druse formation. Hydrothermal origin of druses in cavities of pegmatite veins is universally accepted at present.

Keeping in mind the above relations of the components in druses and in the pegmatoid zone, the latter being adjacent to the druse zone, it is hardly to be doubted but that the origin of the pegmatoid aggregate is likewise the result of the same process of formation. Analogies may be found in innumerable ores, quartz, and other veins, and in the deposition of chalcedony grading into crystals of quartz, etc. It might be inferred that druses and pegmatoid aggregates in pegmatite veins have resulted from the same hydrothermal process.

If we admit that the pegmatite under discussion has resulted from the crystallization of a magma according to the principle of a closed physical-chemical system, we are faced with the contradiction of the development of large grains during the crystallization of a limited amount of magma with a small reserve of heat. A general explanation of this phenomenon on the basis of an abundance of volatile components in the magma in this case cannot hold as all evidence leads us to the conclusion that there was no large excess of mineralizers but rather a deficiency during the formation period of this vein.

A similar conclusion may be reached by studying the relations between the components of the pegmatoid and graphic zones. The formation process of these zones was entirely a hydrothermal one.

The structure of graphic intergrowths is in conformity with this view. F. L. Hess (3) demonstrated that the radial orientation of crystals in pegmatites is due to their metasomatic origin. The orientation of the quartz rods in the pegmatites is in strict agreement with Hess' statement. Concentric sub-zones, described above, are none other than zones of the simultaneous growth of feldspar grains and quartz rods.

Synchronous variations in the thickness of the quartz rods, independent of the direction they intersect feldspar crystals, point to the simultaneous growth of both minerals. No evidence was found of the subsequent intrusion of quartz rods into the feldspar, either in field observation or under the microscope.

In general, the formation of the vein in question took place in the following manner. In the first stage, the aplite dike was formed, perhaps by crystallization of a magmatic intrusion into granite fractures. The crystallization of this material was rapid and having begun at the walls of the fracture it extended into the dike toward the bilateral plane. As the solidification of the aplitic material was taking place the concentration of the volatile constituents originally present in the magma was increasing in the residue of the latter. Finally, there was left a solution differing greatly in its composition from the original magma. The mineral constituents of the vein suggest that the composition of the solution was not a complex one. Probably it was an aqueous alkaline solution with a small amount of fluorine. We have no definite indication of the phase status of this solution, but it is quite probable that it represented a liquid amply saturated with gases. Toward the end of the aplite crystallization the gas pressure had been so increased that the solution began circulating and it resulted in the formation of pegmatite. The bulk of the solution moved along the bilateral plane of the vein, but some of it penetrated into the consolidated aplite, dissolving some of the aplite which was deposited later. Druses were formed in open cavities, but the bulk of the consolidated aplite underwent recrystallization. Thus, the process of pegmatite formation cannot be called metasomatic as no interchange of material took place in the process. The process may be defined as a recrystallization of aplite to form pegmatite. With increased distance from the bilateral plane, the lower became the temperature and the impregnation of the solution into the aplite decreased.

The concentration of the solution depends on the amount of the solvent, the latter being dependent on the rate of diffusion which in turn depends on the pressure and the temperature. As would be expected the formation process of the vein in question was controlled by the three factors of the physical-chemical system, namely, temperature, pressure and mineral concentration. It is evident that the modification of the pegmatite texture also depends on these same three factors. The zonal structure of the vein indicates a change of the physical-chemical factors, the texture of each zone being in accordance with a definite relationship existing between them.

Attempts to determine the quantitative value of these factors favorable to pegmatite formation encounter great difficulties and the results obtained are not exact. There are no criteria for determining the pressure that existed in the process of pegmatite formation. However, keeping in mind that the depth of the pegmatite vein formation was 2–3 kilometers, the pressure must have been considerable.

In regard to the temperature distribution in the vein during the process of formation, the following considerations may be stated. The greater portion of the solutions was following the direction of least resistance, that being the bilateral plane of the vein. Thus, there was a continuous source of heat and the temperature in the zone of druse formation was kept at a fixed level. Solutions diffused into the next zone—the zone of pegmatoid formation—in rather small amounts. Because of that fact the temperature here depended largely on the temperature of the aplite and was accordingly lower. The same may be said about the graphic intergrowth zone, but its temperature was still lower as it was farther from the main channel. This was the lowest temperature zone of the pegmatite vein.

The following observations may help in explaining this fact. Besides the pegmatite veins there are many aplite dikes in Gold Mountain. These rocks consist of quartz, potash feldspar, and albite with some brown and white micas. They have an aplite texture. In these aplite dikes are numerous epigenetic features. These are of three types. In cracks there was observed a yellowish-green aggregate—cookeite with a small amount of hematite scales. Also observed in the dikes were inclusions of pegmatoid aggregates which are clearly apparent, due to their coarse-grained texture. The pegmatoid inclusions consist of quartz, and potash feldspar with a small amount of albite, and show a zonal character free from cavities. The contact between the pegmatoid inclusions and aplite is sharp, and both rocks appear as if fused together. The pegmatoid bodies are lens- and vein-shaped but often are of irregular form. Sometimes cracks can be seen in the aplite that served as main channels for solutions that have formed the above described pegmatoid bodies.

The most interesting phenomenon, however, is the following: sometimes the aplite dikes are corroded and contain cavities that resemble worm-eaten wood. These cavities have capricious shapes and are lined on the inside with druses of albite on which at times are perched quartz crystals, and occasionally cookeite rosettes. The quartz crystals are perfectly transparent, golden colored and beautifully facetted with the common forms. Both ends of these crystals are similarly developed, the crystals being attached to albite by their prism faces.

There is no doubt but that all these phenomena are the result of the same process involving pneumatolytic-hydrothermal solutions in the solidified aplite dikes. Their close proximity to the pegmatite veins indicates an origin from the same source.

Cavities in the aplite originated from the activity of solutions. Material was undoubtedly taken from the same aplite dikes. But it is interesting to note that only albite was deposited while the entire potash feldspar and nearly all the quartz have been carried away. In technology this process is known as fractional-distillation. The separation of the components during such a process depends on the difference in volatility of the components and the selected temperature. The compounds of potash are known to be more volatile than those of sodium. Hence, the phenomenon may take place in aplites at a temperature that would separate these silicates of the alkalies during the fractional-distillation process, under a high pressure.

According to the experiments of N. I. Hitarof and L. A. Ivanof (4) 1 cu. meter of H_2O vapor at about the critical temperature can transport 2.5 kilograms of K_2SiO_3, or 18 kgs. of Na_2SiO_3. Therefore, alkalies will not separate either at this temperature or at one higher than the critical temperature. Consequently, the temperature of their differentiation must be lower than the critical point of the alkaline siliceous solution.

Returning to the pegmatite vein, it should be noted that there are no traces of the transfer of material, in any considerable amount, either in the pegmatoid or in the graphic zones. There are no signs of stratification of mineral constituents or of their preferable growth in any definite direction. The whole structure of the aggregates, on the contrary, brings us to the conclusion that the transformation of aplite into pegmatite took place in situ. Somewhat more extensive transfer took place in the druse formation zone, however, but this transfer was also quite negligible.

If this be true, then the temperature of druse formation in the pegmatites is lower than that of alkali silicate differentiation during the process of fractional distillation. The temperatures of the pegmatoid and graphic granite formations were consequently still lower.

The concentration may be considered as having taken place in the following manner. The concentric sub-zones in the graphic intergrowth are none other than the zones of simultaneous growth of feldspar and quartz crystals. No evidence has been found in the pegmatites in question to favor W. T. Schaller's contention that a subsequent metasomatic intrusion of quartz rods took place into the feldspar matrix. There is also no evidence that feldspar had originated in the form of fine-grained aggregates during the first stage of graphic intergrowth and that later on it recrystallized into coarse grains.

The existence of sub-zones in the graphic intergrowths indicates variation of the physical-chemical conditions during the process of their formation. However, these affected only the quartz. According to C. S. Hitchen's experiments (5) the solubility of SiO_2 in water under conditions analogous to those of N. I. Hitarof's experiments is 0.22 parts in 100 parts of water.

Apparently this was the reason for the zonal structure of the graphic intergrowths. Metasomatic solutions penetrated the aplite non-uniformly, in other words by impulses. A slight deficit of the latter has produced a high supersaturation of the solution with silica, the quartz crystallizing in the form of thin needles. The subsequent addition of solvent lowered the silica concentration and resulted in formation of thicker rods. It is evident that variations in the amount of the solvent were so insignificant that they had no effect on the concentration of the more soluble alkalies, for the feldspar grains grew to 20 cm. in diameter in the same period. The graphic intergrowth was formed in the peripheral zone of the vein where the variations mentioned above were quite likely, since there always was some excess of the solvent in the pegmatoid zone, which was next to the main channel. Accordingly, the pegmatoid texture is uniform and both its components grew to equally large grains.

A. E. Fersman (6) is of the opinion that the quartz and feldspar of the graphic intergrowths are the result of the simultaneous growth of both minerals. He looks for simple crystallographic relations between the components and offers a law of quartz and feldspar intergrowth in "graphic granites" known as the Fersman's law.

In 1925 N. N. Gornostaev (7) and in 1938 L. A. Kosoy (8) also offered their laws relating to these intergrowths.

The elongated form of the quartz rods is explained by Fersman as due to the inductive influence of the growing feldspar crystal facets on the growing crystals of quartz.

It can be easily shown that the simultaneous growth of quartz and feldspar cannot in itself be the cause of a graphic texture. In the pegmatoid zone, and in many other cases, these minerals grow simultaneously for the most part, but there is no evidence of a graphic texture. The failure of simple crystallographic laws in graphic intergrowth has been established by E. E. Wahlstrom (9) who proved that such laws do not exist at all. This conclusion is confirmed by the above described relations between quartz and feldspar in the pegmatites of Gold Mountain.

The inductive influence may be said to have really taken place, though the inducting element was not a feldspar facet, but the mobile plane of separation between the aplite and the growing graphic intergrowth. This plane during the process of penetration by metasomatic solutions into the aplite moved towards the latter so as to elongate the quartz rods along with the movement. In this case the plane was of spherical form and that is why the rods growing as it moved are normal to it and have formed a radial structure.

SUMMARY AND CONCLUSIONS

The pegmatite veins of Gold Mountain with accompanying graphic granite have originated by a pneumatolytic-hydrothermal transformation of aplite dikes. The active agents in this process were aqueous siliceous alkaline solutions containing a small amount of fluorine. These solutions originated from the volatile components originally contained in the aplite substratum and from the mother liquor of the granite magma.

The physical-chemical conditions of formation of the zones constituting the pegmatite vein involved high pressure but the temperature was below the critical point of the aqueous siliceous alkaline solution, and the concentration of silica and alkalies reached the point of supersaturation. The transfer of material during the pegmatite formation was insignificant. The various factors may be detailed for the separate zones as follows:

Zones	Temperature	Pressure	Degree of supersaturation		Transfer
			With SiO_2	With alkalies	
Druses	High	High	Low	Low	Intensive
Pegmatoid	Medium	Medium	Moderate	Moderate	Weak
Graphic granite	Low	Low	High	Moderate	Insignificant

The absence of any simple crystallographic law of orientation in the quartz and feldspar graphic intergrowths is confirmed.

The inductive influence was present during the growth of the quartz rods and it is established that the inducting agent was not a crystallographic element of the feldspar, but the mobile plane of separation between the aplite and growing graphic intergrowths.

If we free ourselves from the traditional concept that graphic intergrowths of quartz and feldspar are a specific magmatic phenomena, then several more or less mysterious phenomena may be satisfactorily explained.

One of such unsolved riddles is the presence of pegmatite lenses in the norite of the nickel-bearing eruptive rock at Sudbury. This riddle cannot be solved if the magmatic origin of graphic granite is a condition sine qua non. But following the view expressed in this article, this phenomenon may also be easily explained. A combination of physical-chemical conditions corresponding to the zone of graphic granite involving circulating solutions is easily imaginable. Such solutions can transfer and deposit the corresponding substances in a proper form and in the same way in which the formation of quartz, barite, and other vein minerals has taken place. The pegmatite-forming solutions may not be related to the rocks enclosing the pegmatite.

Certain petrographic phenomena are also clarified. A. N. Zavaritsky (10), who has investigated the nature of the Ural rapakivi, says: "In two samples of rapakivi granite micropegmatitic intergrowths are restricted to the contact between large grains of quartz and those of feldspar, and are similar to the phenomenon pointed out by Polkanof, Laitakari, and Beliankin as secondary micropegmatites found at the contact of the granite with diabase dikes."

This phenomenon may be explained as follows: the granite already solidified, may have been subjected to a strong pressure and begins to melt. When liquid drops of a quartz-feldspar composition appear in some places in the rock, the pressure may cease and these drops crystallize according to the eutectic principle into graphic intergrowths. This complicated explanation, however, is not likely to be true and lacks proof.

The writer thinks that a granophyr is also the product of metasomatic activity. Some points in favor of this view are the following: (a) The structure of the micropegmatite intergrowths in the rapakivi of Berdiaush. There they form at the boundary between the quartz and feldspar grains and as deep penetrations into the grains of quartz and feldspar. Micropegmatite intergrowths occur also between the nucleus of the orthoclase and the oligoclase shell. (b) The relationship of the diabase dike to the granophyrous portion of the granite, as was emphasized by Zavaritsky. (c) The conception of graphic intergrowth genesis as presented in this paper. (d) The interpretation of rapakivi texture by Zavaritsky who states that it originates as the result of the granite being acted upon by the metasomatic activity of solutions diffusing through it.

The writer suggests that the presence of granophyre in granite can be considered, in general, as evidence of metasomatic activity in the process of granite formation.

ACKNOWLEDGMENT

This paper is an attempt to expand the ideas of Frank L. Hess and Waldemar T. Schaller (11) on the genesis of pegmatites. The writer has

used his conception for the explanation of some petrographic phenomena, being quite convinced of the truth of the conclusions reached and expressed in Schaller's presidential address.

References

1. Campbell, I., Alpine mineral deposits: *Am. Mineral.*, **12,** 157–167 (1927).
2. Koenigsberger, J., Die Minerallagerstätte in Biotitprotogin der Aarmassivs: *N. Jahrb. Min.*, Bd. **14,** 43.
3. Hess, Frank L., The natural history of the pegmatites: *Eng. and Min. Journ. Press*, **120,** No. 8, 289–298 (1925).
4. Хитаров, Н. И. и Иванов, Л. А. Исследование в области крити критических температур водных растворов. Труды II Совещания по экспериментальной минералогии и петрологии Москва (1937).
5. Hitchen, C. S., A method for the experimental investigation of hydrothermal solutions with notes on application to the solubility of silica: *Trans. Inst. Min. and Met.*, **44,** 255–280 (1935).
6. Ферсман. А. Е. Пегматиты (1940).
7. Горностаев, Н. Н. О новых эаконах полевошпато кварцевого срастаиия. Иэвстия Томского Технологического Иистиута 46, стр. I (1925).
8. Косой, Л. А. Срастание кварца иполевых щпатов иэ пегматитовых жил Карелии. Доклады Академии Наук, 275 277 (1938).
9. Wahlstrom, E. E., Graphic granite: *Am. Mineral.*, **24,** 681–698 (1939).
10. Zavaritsky, A., Petrography of the Berdiaush pluten: *Trans. Centr. Geol. and Prosp. Inst.*, Fas **96,** 353 (1937) U.S.S.R.
11. Schaller, Waldemar T., Mineral replacement in pegmatites: *Am. Mineral.*, **12,** 59–63 (1927).

PREPARATION AND PROPERTIES OF SOME COMPOUNDS IN THE SYSTEM $H_2O–Na_2O–P_2O_5$

EARL INGERSON AND GEORGE W. MOREY,
Geophysical Laboratory, Carnegie Institution of Washington.

ABSTRACT

Optical properties of all known compounds of Na_2O and P_2O_5, both hydrous and anhydrous, are given. For eight of these the data are taken entirely from the literature; eight more have been re-studied; five are here described optically for the first time. Crystallographic and density data are given for some of them.

The methods of preparing twelve of these compounds are given, and for the others methods can be obtained from the literature cited. The nomenclature of these phosphates is discussed. Refractive indices are given for eleven glasses in the system $NaPO_3-Na_4P_2O_7$.

The voluminous literature dealing with the system $H_2O–Na_2O–P_2O_5$ contains descriptions of numerous ternary compounds, together with a large amount of speculation as to the constitution of these compounds and of their aqueous solutions. Much of this speculation about the constitution of solutions is not well founded and postulates hypothetical acids, the existence of which is supported by no real evidence. Nevertheless, some of these solutions do present striking illustrations of the difference in properties of solutions stoichiometrically equivalent, but of different histories. The mass action of water in such solutions ultimately causes them to become identical in properties, but the rate of this change commonly is slow at ordinary temperatures. It is, however, rapidly accelerated by increasing temperature, and the work of Abbot (1) demonstrated that the change to what is described as the orthophosphate condition, which takes months at ordinary temperatures, is complete in a short time at the boiling point.

We thus have in this system the possibility of realization of conditions of metastable equilibrium, and from the exhaustive study of such metastable solutions there appears a possibility of making a real contribution to the general problem of the constitution of liquids in general. An illustration is to be found in the binary system $H_2O–2Na_2O \cdot P_2O_5$, that is, with solutions in which the ratio of Na_2O to P_2O_5 is that of a disodium phosphate. In the series stable at ordinary temperatures there are the following compounds: $Na_2HPO_4 \cdot 12H_2O$ ($2Na_2O \cdot P_2O_5 \cdot 25H_2O$), $Na_2HPO_4 \cdot 7H_2O$ ($2Na_2O \cdot P_2O_5 \cdot 15H_2O$), and $Na_2HPO_4 \cdot 2H_2O$ ($2Na_2O \cdot P_2O_5 \cdot 5H_2O$). Each of these compounds has an incongruent melting point, and in each the solubility increases with temperature. The final compound of this series is Na_2HPO_4 ($2Na_2O \cdot P_2O_5 \cdot H_2O$), the solubility curve of which is strongly retrograde and must terminate at some unknown quadruple point at which the anhydrous compound, $Na_4P_2O_7$ ($2Na_2O\cdot P_2O_5$), is one of the coexisting crystalline phases. When this anhydrous compound is dissolved in water and the solution allowed to evaporate at ordinary temperature, the compound customarily written as $Na_4P_2O_7\cdot 10H_2O$ ($2Na_2O\cdot P_2O_5\cdot 10H_2O$) separates. This compound is metastable with respect to the preceding series, and its solution, on long standing or on heating, becomes transformed into one from which one of the compounds of the preceding series will separate. The solubility curve of the 10-hydrate will intersect the metastable prolongation of the solubility curve of $Na_4P_2O_7$ below the quadruple point $Na_4P_2O_7$–Na_2HPO_4–L–V, giving rise to a metastable quadruple point $Na_4P_2O_7$–$Na_4P_2O_7\cdot 10H_2O$–L–V,

Table 1. Optical Properties of Compounds

Formula	2V	Sign	α	ω	β	ε	γ
Ratio $Na_2O:P_2O_5=3:1$							
$Na_3PO_4\cdot 12H_2O$(4)		+		1.4458		1.4524	
$Na_3PO_4\cdot 7H_2O$*	85°	+	1.462		1.470		1.478
$Na_3PO_4\cdot H_2O$(10)*		+		1.497		1.522	
Na_3PO_4(10)	76°	+	1.493		1.499		1.508
Ratio $Na_2O:P_2O_5=2:1$							
$Na_2HPO_4\cdot 12H_2O$(4)	57°	−	1.432		1.436		1.437
$Na_2HPO_4\cdot 7H_2O$(4)	39°	+	1.4412		1.4424		1.4526
$Na_2HPO_4\cdot 2H_2O$*	*ca.* 80°	+	1.450		1.461		1.477
Na_2HPO_4*	78°	+	1.483		1.499		1.525
$Na_4P_2O_7$(17)*	40°	+	1.475		1.477		1.496
$Na_2P_4O_7\cdot 10H_2O$(3),(4)	60½°	+	1.4499		1.4525		1.4604
Ratio $Na_2O:P_2O_5=5:3$							
$Na_5P_3O_{10}$ I(17)*	21°	+	1.477		1.478		1.504
$Na_5P_3O_{10}$ II(17)*	57°	+	1.470		1.477		1.502
$Na_5P_3O_{10}\cdot 6H_2O$(16)*	20°	+	1.449		1.450		1.482
Ratio $Na_2O:P_2O_5=1:1$							
$NaH_2PO_4\cdot 2H_2O$(2),(4)	82°	−	1.4400		1.4625		1.4818
$NaH_2PO_4\cdot H_2O$(4)	29°	−	1.4557		1.4852		1.4873
NaH_2PO_4*	64°	−	1.481		1.507		1.517
$NaPO_3$ I(14),(17)*	80°	−	1.474		1.478		1.480
$NaPO_3$ II(17)*	78°	+	1.498		1.510		1.529
$NaPO_3\cdot 2H_2O$(15)*			1.432				1.441
$Na_2H_2P_2O_7$*			1.510				1.517
$Na_2H_2P_2O_7\cdot 6H_2O$(3),(4)	32°	−	1.4599		1.4645		1.4649

Numbers in parentheses are those of references at end of paper.

* Studied by Ingerson.

provided that no hydrate of $Na_4P_2O_7$ containing less than 10 molecules of water exists. Similar complex reactions are to be found with other ratios of $Na_2O:P_2O_5$. It appeared to us that the entire relationship of the various compounds in the ternary system H_2O–Na_2O–P_2O_5 could best be cleared up by the determination of the phase equilibrium relationships in the system up to the temperatures at which the anhydrous crystalline compounds become the stable solid phases. This research was started, but has been interrupted by the pressure of war work. Accordingly, it seems desirable to place on record a few qualitative observations, as well as the optical descriptions of some of the compounds we have prepared.

Most of the data heretofore available on the phosphates of sodium are contained in articles by Dufet and by Joly and Dufet (2, 3, 4). The accompanying table summarizes the optical properties of all the sodium phosphates of which we have a record, and in the notes which follow are comments on the preparation of these compounds. The new measurements include fair to good data on several sodium phosphates that have not been described optically before, and we have checked and extended measurements on a few others. Where two compounds have quite similar indices, as $Na_5P_3O_{10}$ I and $Na_5P_3O_{10}$ II, the properties were measured very carefully in sodium light, but the properties of a compound quite different from any of the others were determined much more roughly. Our opinion of the relative merits of the various determinations is indicated in the following notes.

NOTES ON THE VARIOUS COMPOUNDS

Ratio $Na_2O:P_2O_5=3:1$

$Na_3PO_4\cdot 12H_2O$. Density 1.645. Melts incongruently at $70.75\pm.01°$ (D'Ans and Schreiner, 5), but they did not identify the solid phase formed, which probably was $Na_3PO_4\cdot 7H_2O$. May exist in two forms, one of which is of variable composition (Menzel and Sahr, 6).

"$Na_3PO_4\cdot 10H_2O$." Mentioned as "easily prepared," isotropic by Baker (7), but shown by Mason and Ashcraft (8) to be $NaF\cdot 2Na_3PO_4\cdot 19H_2O$.

$Na_3PO_4\cdot 8H_2O$. Also mentioned by Baker, but not obtained by us or other investigators.

$Na_3PO_4.7H_2O$. Prepared by evaporation of a solution of Na_3PO_4 at 83°; also obtained by Hall (9), who gives a good analysis but no properties. Properties measured in white light without measuring the indices of the oils on a refractometer at the time the determinations were made. Indices probably ± 0.002. Beta was determined from alpha, gamma, and 2V, which was measured on the universal stage.

$Na_3PO_4 \cdot H_2O$. Measurements about like those for the 7 hydrate. Obtained by evaporation at 86° of a solution of 100 g. $Na_2HPO_4 \cdot 12H_2O$ and 50 g. NaOH. Analysis of material which probably contained some adhering mother liquor gave 16.6 per cent H_2O; $Na_3PO_4 \cdot 2H_2O$ contains 18 per cent; $Na_3PO_4 \cdot H_2O$, 9.9 per cent. Schroeder, Berk and Gabriel (10) give $\omega = 1.498$, $\epsilon = 1.525$ for crystals of $Na_3PO_4 \cdot H_2O$, without giving evidence of how the composition was determined.

Na_3PO_4. Schroeder, Berk and Gabriel (10) describe anhydrous sodium orthophosphate as monoclinic, 2V calculated from indices; $\rho > v$, distinct; b = acute bisectrix; $V \wedge c = 10° \pm$. Crystals described show 100, 110, and 001 faces. Twinning on 100 said to be common. They give the solubility curve of Na_3PO_4 from 80° to 350°C.

Ratio $Na_2O:P_2O_5 = 2:1$

$Na_2HPO_4 \cdot 12H_2O$. Monoclinic. $a:b:c = 1.732:1:1.416$. $\beta = 58°36'$. $110 \wedge 1\bar{1}0 = 67°56'$. Dispersion $\rho < v$. Density 1.531.

$Na_2HPO_4 \cdot 7H_2O$. Monoclinic. $a:b:c = 2.871:1:1.859$. $\beta = 83°3'$. $110 \wedge 1\bar{1}0 = 79°48'$. Dispersion $\rho > v$. Density 1.679.

$Na_2HPO_4 \cdot 2H_2O$. Formed by evaporation of solution at 60°. Indices measured in white light, probably ±0.002. Beta calculated from alpha, gamma, and 2V, which was measured on the universal stage. Composition checked by loss in weight.

Na_2HPO_4. Formed by evaporation at 105°. Composition checked by loss in weight. Indices measured in white light, probably ±0.002. Beta calculated from alpha, gamma, and 2V, which was measured on the universal stage.

The solubility curve of Na_2HPO_4 in water has been studied by Menzies and Humphrey (11) and by Hammick, Goadby, and Booth (12). The incongruent melting points as given by them are, respectively: 12Aq, 35.2° and 35°; 7Aq, 48.3° and 48.09°; 2Aq, 95° and 94.97°. Hammick, Goadby, and Booth give evidence indicating that there are two forms of the 12-hydrate, with a transition at 29.6°. No crystallographic or optical details are given in either of the above references.

$Na_4P_2O_7$. Beta calculated from alpha, gamma, and 2V, which was measured on the universal stage.

$Na_4P_2O_7 \cdot 10H_2O$. Obtained by evaporation at room temperature of a solution of $Na_4P_2O_7$ in water. Monoclinic. $a:b:c = 1.287:1:1.895$. $\beta = 81°44'$. $110 \wedge 1\bar{1}0 = 76°16'$. Axial plane $\perp 010$. Dispersion $\rho > v$. Density 1.815.

Ratio $Na_2O:P_2O_5 = 5:3$

$Na_5P_3O_{10}$ I and II. These compounds were made by melting $NaPO_3$

and $Na_4P_2O_7$ in proper proportions and cooling. If the furnace and charge were cooled to room temperature, by cutting off the furnace current, the I-form was usually obtained, and the II-form by removing the crystallized melt at from 500 to 550°. The inversion to the II-form was always accompanied by spontaneous powdering. The relationship between these two forms is not clear. Refractive indices were measured with sodium light, and the oils used were checked on a refractometer at the same temperature and using the same light source. The axial angles were measured on the universal stage, using sodium light. The observed values of 2V agree closely with the values calculated from the indices, which are probably accurate in the third place, 2V to the nearest degree.

$Na_5P_3O_{10} \cdot 6H_2O$. Obtained by dissolving crystalline $Na_5P_3O_{10}$ in water and evaporating at room temperature. The crystals were separated from mother liquor by suction on a sintered glass filter, and crystals and solution analyzed. The crystals gave 44.80 per cent P_2O_5; theory 44.75. The solution represented 45 per cent of the $Na_5P_3O_{10}$ taken, and contained 0.165 g. $Na_5P_3O_{10}$, or 0.213 g. $Na_5P_3O_{10} \cdot 6H_2O$ per gram of solution, the solubility at "room temperature," about 25°. The P_2O_5-content per gram of solution was 0.0945.

When a melt containing more $NaPO_3$ than corresponds to $Na_5P_3O_{10}$, say 43.4 per cent $NaPO_3$ and 56.6 per cent $Na_4P_2O_7$, was quickly cooled to a glass, powdered, dissolved in hot water, and the solution allowed to evaporate at room temperature over sulfuric acid, it dried to a gummy-to-hard glass. When the cooling was so carried out that the product consisted of glass and crystals of $Na_4P_2O_7$, crystals of $Na_4P_2O_7 \cdot 10H_2O$ immersed in a thick, viscous liquid were obtained. When the cooling was so carried out that the product consisted of glass and crystals of $Na_5P_3O_{10}$, the evaporation yielded crystals of $Na_5P_3O_{10} \cdot 6H_2O$ surrounded by liquid too viscous to be separated completely from the crystals, which were identified by their optical properties. Finally, when the cooling was so carried out that the product was completely crystallized to a mixture of $NaPO_3$ and $Na_5P_3O_{10}$, crystals of $NaPO_3 \cdot 2H_2O$ and $Na_5P_3O_{10} \cdot 6H_2O$ were obtained. The above sequence of striking differences in behavior depending on the thermal history of the material which was dissolved to make the aqueous solutions indicates that in the glassy phase there are no "molecular groupings" which on solution give rise to crystals of the several hydrated compounds. It should also be mentioned that each of the above solutions on sufficient boiling will give solutions from which hydrates of NaH_2PO_4 and Na_2HPO_4 will crystallize.

The indices of $Na_5P_3O_{10} \cdot 6H_2O$ were measured in sodium light, probably to ±0.001. When well crystallized it has blocky cleavage in two directions at 90°. When precipitated from solution by alcohol the crystals are intricately twinned in such a manner that γ is difficult to observe. Dispersion, $\rho > \upsilon$.

Ratio $Na_2O:P_2O_5 = 1:1$

$NaH_2PO_4 \cdot 2H_2O$ and $NaH_2PO_4 \cdot H_2O$ are the two commonly obtained hydrates, with incongruent melting points at 40.8° and 57.4°, respectively. NaH_2PO_4 was prepared by evaporation at 95°, and in experiments in closed vessels it was obtained up to 300°. However, at this temperature it looked as if the compound had melted congruently, then solidified. With smaller water contents, $NaPO_3$ II was obtained, sometimes in excellent crystals.

$NaH_2PO_4 \cdot 2H_2O$. Orthorhombic. $a:b:c = 0.915:1:1.569$. $110 \wedge 1\bar{1}0 = 95°6'$. Density = 1.910.

$NaH_2PO_4 \cdot H_2O$. Orthorhombic. $a:b:c = 0.934:1:0.962$. $110 \wedge 1\bar{1}0 = 93°56'$. Dispersion, $\rho < \upsilon$. Density = 2.055.

NaH_2PO_4. Indices measured in white light; probably ±0.002. 2V was measured on the universal stage in white light.

$NaPO_3$ *I*. The discussion of the forms of $NaPO_3$ is made more difficult by the persistence of the now absurd system of nomenclature devised almost one hundred years ago by Fleitmann and Henneberg (13), which not only has no justification in modern theory but also is in conflict with modern knowledge of the structure of crystals and glasses. The glassy form, called "sodium hexametaphosphate," is but one of a continuous series of glasses in which the assumption of definite compounds is in conflict with modern theories of the structure of glasses. The characterizations of the soluble crystalline form, $NaPO_3$ I, as sodium trimetaphosphate, and of the insoluble $NaPO_3$ II as sodium monometaphosphate are likewise in conflict with our knowledge of crystal structure, in which such molecular aggregations play no part.

$NaPO_3$ *I* is obtained by crystallizing $NaPO_3$ just below the melting-point. The indices were measured in sodium light, probably ±0.001; 2V was measured on the universal stage.

$NaPO_3$ *II* may be obtained by crystallizing the glass at about 450°, but the best crystals were obtained by hydrothermal means, as mentioned above. The indices were measured in sodium light and the oils checked on the refractometer, and are probably accurate in the third decimal place. 2V was measured on the universal stage. It is probably orthorhombic, $110 \wedge 1\bar{1}0$ very nearly 90°, $110 \wedge 101$ *ca.* 55°. Axial plane parallel to 010, acute bisectrix parallel to a-axis.

$NaPO_3 \cdot 2H_2O$. This was prepared by dissolving $NaPO_3$ I in water and evaporating over H_2SO_4. The crystals were not very satisfactory. The indices are no better than ±0.003, and the high index possibly not that good. Universal stage determinations showed most of the grains to be essentially uniaxial and negative, but a few of them gave values of 2V of approximately 80°, both positive and negative. These were probably grains of the two anhydrous forms, $NaPO_3$ II and I, respectively.

$Na_2H_2P_2O_7$. Material was very fine needles with positive elongation. The indices given are really α' and γ', since it was not possible to check the orientation of the needles.

$Na_2H_2P_2O_7 \cdot 6H_2O$. This was not prepared by us. Monoclinic, $a:b:c = 2.026:1:2.049$. $\beta = 56°41'$. $110 \wedge 1\bar{1}0 = 61°8'$. Dispersion, $\rho < \upsilon$, strong.

REFRACTIVE INDICES OF GLASSES

Refractive indices of several sodium phosphate glasses were measured by preparing mixtures of oils to match the glasses in sodium light. The indices of the glasses were then measured on the refractometer. Indices are given to four places, but the fourth place is probably almost entirely without significance because a given glass may vary considerably in index with different heat treatments. The glasses were not annealed, but allowed to cool freely in air, usually in 10-gram lots in the 15-cc. platinum crucible in which they were melted. Following are the compositions, given as weight fractions $Na_4P_2O_7$ in the binary system $NaPO_3$—$Na_4P_2O_7$, followed by their respective indices, n_D: 0 ($NaPO_3$) 1.4847; 0.15, 1.4846; 0.33, 1.4845; 0.40, 1.4843; 0.45, 1.4836; 0.475, 1.4834; 0.50, 1.4831; 0.5659, 1.4825; 0.57, 1.4823; 0.60, 1.4820; 0.72, 1.4814.

REFERENCES

1. ABBOT, G. A., The rate of hydration of pyrophosphoric acid in aqueous solution: *Jour. Am. Chem. Soc.*, **31**, 763–770 (1909).
2. JOLY, A., AND DUFET, H., Sur l'orthophosphate et l'arséniate monosodiques: *Bull. soc. min. France*, **9**, 194–201 (1886).
3. DUFET, H., Sur la forme cristalline des pyrophosphates et hypophosphates de soude: *Bull. soc. min. France*, **9**, 201–210 (1886).
4. DUFET, H., Étude cristallographique et optique des phosphates, arséniates et hypophosphates de soude: *Bull. soc. min. France*, **10**, 77–120 (1887).
5. D'ANS, J., AND SCHREINER, O., Die ternären Systeme Alkali—Phosphorsäure—Wasser: *Zeits. Phys. Chem.*, **75**, 95–107 (1910).
6. MENZEL, HEINRICH, AND VON SAHR, ERNST, Studien an Alkaliphosphaten und -Arsenaten; II, Tertiäres Natriumphosphat: *Zeits. Elektrochem.*, **43**, 104–119 (1937).
7. BAKER, HARRY, The ortho-vanadates of sodium and their analogues: *Jour. Chem. Soc., Trans.*, **47**, 353–361 (1885).
8. MASON, C. W., AND ASHCRAFT, E. B., Trisodium phosphate—sodium fluoride; Phase studies and analytical methods: *Ind. Eng. Chem.*, **31**, 768–774 (1939).
9. HALL, JOHN A., Some analogous phosphates, arsenates, and vanadates: *Jour. Chem. Soc.*, **51**, 94–97 (1887).

10. Schroeder, W. C., Berk, A. A., and Gabriel, Alton, Solubility equilibria of sodium sulfate at temperatures from 150 to 350°. III. Effect of sodium hydroxide and sodium phosphate: *Jour. Am. Chem. Soc.*, **59**, 1783–1795 (1937).
11. Menzies, A. W. C., and Humphrey, Ed. C., Disodium monohydrogen phosphate and its hydrates. Their solubilities and transition temperatures: *VIII Int. Cong. Appl. Chem.*, **2**, 175–178 (1912).
12. Hammick, D. L., Goadby, H. K., and Booth, Henry, Disodium hydrogen phosphate dodecahydrate: *Jour. Chem. Soc.*, **117**, 1589–1592 (1920).
13. Fleitmann, Th., and Henneberg, W., Ueber phosphorsäure Salze: *Liebig's Annalen der Chemie*, **65**, 304–334 (1848).
14. Beans, H. T., and Kiehl, S. J., Sodium monometaphosphate and its acid hydration: *Jour. Am. Chem. Soc.*, **49**, 1878–1891 (1927).
15. Kiehl, S. J., and Coats, Harvey P., The hydration of sodium monometaphosphate in alkaline solution at 75°: *Jour. Am. Chem. Soc.*, **49**, 2180–2193 (1927).
16. Bonneman, P., and Brassiere, M., Condensed phosphoric acids. Polyphosphates: *Compt. rend.*, **206**, 1379–1380 (1938).
17. Partridge, Everett P., Hicks, Victor, and Smith, G. W., A thermal, microscopic, and *x*-ray study of the system $NaPO_3$–$Na_4P_2O_7$: *Jour. Am. Chem. Soc.*, **63**, 454–466 (1941).

AUTORADIOGRAPHY OF MINERALS

CLARK GOODMAN AND GEORGE A. THOMPSON,[1]
Massachusetts Institute of Technology
Cambridge, Massachusetts.

ABSTRACT

Using stray slow neutrons from the cyclotron on elements having large nuclear cross-sections for neutron reactions (n, γ) and yielding radioactive isotopes of convenient half-periods, autoradiographic studies of a number of common minerals have been made. The locus and relative concentrations of the activated elements in these minerals are determined by placing polished sections of the specimens in direct contact with photographic film. The source of the effective β-radiation is determined from the decay rate and intensity of the activity. A reconnaissance study has been made of minerals containing manganese, gold, copper, tungsten, phosphorus, potassium, barium, sodium and arsenic.

INTRODUCTION

Geologists frequently see direct evidence of natural radioactivity in the pleochroic halos that spot biotite in thin sections. These microscopic discolorations result from alpha-ray bombardment of the mineral immediately surrounding tiny inclusions of radioactive elements. The small size is due to the short range of the alpha rays in the mineral. Substituting photographic plates for the sensitive mineral, Mügge[2] obtained the first autoradiographs of radioactive minerals. Numerous investigators subsequently have used this technique to determine the distribution of uranium and thorium in terrestrial materials.

Recent advances in nuclear physics make it possible to induce radioactivity in all elements. However, alpha rays are rarely emitted by these so-called artificially radioactive elements. Instead they emit beta and gamma rays. Although less effective than alphas, beta rays may be used for broader applications of autoradiography. In the present work only a few of the more obvious applications to geologic materials have been tested. It has been found that the uniform distribution of a particular element in a mineral or its localization in inclusions often can be demonstrated by the method. If the valuable element in an ore is present in minute inclusions, the position may be revealed by the radiations from the induced radioactivity. Thus, fine particles of gold in a quartz matrix or manganiferous laminae or nodules in a shale can be studied by this technique. The information obtained may be of value in the beneficiation of these materials. By means of autoradiography the irregular distribution of elements in zoned minerals can also be studied.

---

[1] Now with U. S. Geological Survey, Terlingua, Texas.

[2] Mügge, O., Radioaktivität und pleocroitische Höfe: *Zentralbl. f. Mineralogie*, **71**, 144–147 (1909).

GENERAL PRINCIPLES

Artificial radioactivity can be produced by bombarding stable atoms with various radiations, i.e., alpha rays, neutrons, protons, electrons, gamma rays, or deuterons. A given intensity of bombardment is capable of producing only a certain maximum induced activity, as equilibrium between the production and disintegration of active atoms is finally reached. This maximum yield is approached at a rate depending upon the half-period of the induced activity. The half-period for activation is the same as that for disintegration. For example, Mn^{56}, the isotope of manganese with atomic weight 56, has a half-period for disintegration of 2.6 hours and under bombardment reaches half its maximum intensity in 2.6 hours. Bombardments longer than about 10 half-periods produce no appreciable increase in activity.

Nuclei of different atomic forms differ in the degree to which they interact with bombarding particles. The probability of interaction can be considered as proportional to the target area presented to the bombarding particles by a given nucleus. This quantity is called the *nuclear cross-section* and is generally expressed in square centimeters. Because of the wave mechanical nature of the interaction, the cross-section may be smaller or larger than the actual nuclear area. The cross-section varies not only with different kinds of bombarding particles but also with the velocity of these particles. In this report only *nuclear cross-sections for the capture of slow neutrons* will be considered.

Neutron bombardment offers certain advantages over direct proton or deuteron bombardment of minerals. First, it is not necessary to prepare the sample in the form of a target, which, due to the energy of the beam, would require thin, water-cooled sections. Second, a flood of neutrons escapes continuously from an operating cyclotron. These by-product neutrons can be utilized at no increase in cost. Third, only one or two samples can be activated simultaneously by direct bombardment, whereas an almost unlimited number can be exposed concurrently to neutrons. Fourth, there are numerous competing reactions involved with deuterons and protons, while the reactions with neutrons, particularly slow neutrons, are quite simple. For these reasons the present research has been limited to neutron activation, and, unless otherwise stated, thermal-velocity neutrons have been used.

SUITABILITY OF ELEMENTS

Following the initial work with manganese minerals,[3] an attempt was made to list the elements in the order of their suitability for autoradiog-

[3] Goodman, C., and Picton, D. C., Autoradiography of ores: *Phys. Rev.*, **60**, 688 (1941).

raphy as determined by their half-periods and cross-sections. The more favorable elements are listed in Table 1 in the order of decreasing suitability, based on the purely arbitrary rating shown in Fig. 1. From the standpoint of cyclotron operations and also the convenience in photographing and measuring the induced activity, elements with half-periods between 1 and 10 hours are preferred, hence are given an *A* rating. Those within the next, or *B*, group have either much shorter half-periods, 0.5 to 1 hour for B_1, or much longer, 10 to 50 hours for B_2. Thus, if the half-period is too long or too short, the suitability decreases accordingly. As we have seen, the larger the capture cross-section, the greater the intensity of induced activity for a given bombardment. Although in some cases difficulty results from an excessive amount of activity, in general the larger the probability of activation, the greater the sensitivity and the more suitable the element for study. Thus a second alphabetical scale is used for cross-sections. The combination of these two ratings determines the relative position of the elements in Table 1.

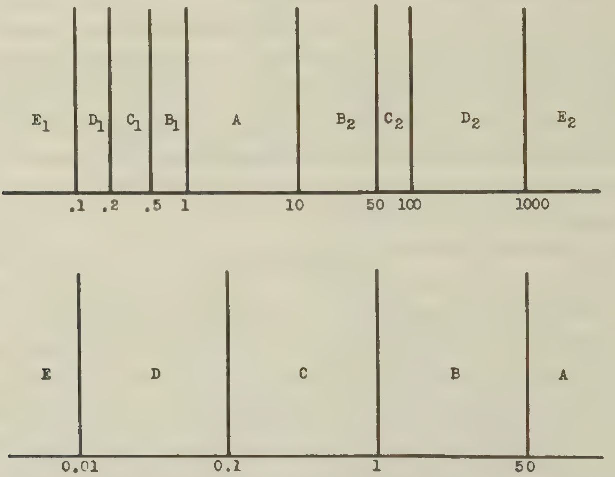

FIG. 1. Arbitrary autoradiographic rating. In the upper diagram is given the alphabetical rating of half-periods, in hours, of the induced radioactivity. The lower diagram evaluates the capture cross-sections for slow neutrons in units of 10^{-24} cm^2.

PROCEDURE

A hand sample (100 to 1000 grams) of the mineral to be studied is ground flat on one face. The final grinding should be with a powder of about No. 304 grade. Polishing is unnecessary, since the objective is merely to have a flat surface for direct contact with the photographic

TABLE 1. AUTORADIOGRAPHIC ELEMENTS

(The elements are arranged in the order of decreasing suitability for autoradiographic study. The dominant radioactive isotopes resulting from slow neutron bombardment are indicated together with their half-periods (d≡days, h≡hours, m≡minutes). The capture cross-sections are average values for the natural isotopic mixtures.)

Element	Radio Isotope	Half-period	Capture Cross-Section for "Average" Atom in 10^{-24} cm^2.	Rating
Dysprosium	Dy^{165}	2.5 h.	440	AA
Europium	Eu^{152}	9.2 h.	260	AA
Barium	Ba^{139}	86 m.	2	AB
Indium	In^{116}	54 m.	119	B_1A
Manganese	Mn^{56}	2.6 h.	9	AB
Arsenic	As^{76}	26 h.	3	B_2B
Copper	Cu^{64}	12.8 h.	1	B_2B
Iridium	Ir^{194}	19 h.	38	B_2B
Lanthanum	La^{140}	31 h.	5	B_2B
Tungsten	W^{187}	24 h.	10	B_2B
Gold	Au^{198}	2.7 d.	130	C_2A
Iodine	I^{128}	25 m.	6.5	C_1B
Platinum	Pt^{199}	31 m.	0.7	B_1C
Potassium	K^{42}	12.4 h.	0.1	B_2C
Sodium	Na^{24}	14.8 h.	0.4	B_2C
Calcium	Ca^{49}	2.5 h.	0.01	AD
Nickel	Ni^{63}	2.6 h.	0.03	AD
Silicon	Si^{31}	2.8 h.	0.02	AD
Yttrium	Y^{90}	60 h.	0.7	C_2C
Chlorine	Cl^{38}	37 m.	0.07	B_1D
Zinc	Zn^{69}	57 m.	0.08	B_1D
Bismuth	Bi^{210}	5 d.	0.1	D_2C
Phosphorus	P^{32}	14.3 d.	0.2	D_2C
Scandium	Sc^{46}	85 d.	2.8	E_2B
Tantalum	Ta^{182}	97 d.	4	E_2B
Vanadium	V^{52}	3.9 m.	5	E_1B
Magnesium	Mg^{27}	10.2 m.	0.03	D_1D
Aluminum	Al^{28}	2.4 m.	0.2	E_1C

film or plate. The specimens are placed in a specially constructed container located as near as possible to the cyclotron target. This container should have paraffin walls* 2 to 3 inches thick. Bombardment proceeds for a few minutes to several hours, depending upon the element under study. The specimens are removed and transferred to the dark room. The flat surfaces are placed on photographic material and exposed for a few minutes to several hours. In the resulting autoradiographs dark areas directly adjoin areas of high induced radioactivity in the specimens and are caused by the interaction of the beta rays with the silver emulsion. Relatively clear areas correspond to inactive portions of the specimens. Thus, photographically, the autoradiographs are negatives. Positive prints can be made either by contact or by enlargement. The illustrations included in this report are all prints. Hence, the light areas correspond to high induced activity, and the dark areas correspond to inactive regions. To aid in the comparison of the autoradiograph with the specimen from which it was produced, a photograph of the flat surface of the mineral is obtained. The print of the direct photograph is made the same size as the print of the autoradiograph. In this manner, direct comparison can be more easily made.

---

* Paraffin is used because it is an inexpensive, hydrogenous solid. The high-velocity neutrons emitted by the target are more completely slowed down by collisions with particles of approximately the same mass, i.e., hydrogen nuclei. Nuclear capture cross-sections are larger for low-velocity neutrons than for the more energetic, fast neutrons.

As indicated in Table 1, the half-periods have a wide range of values and, with a few exceptions, are distinctly different. This characteristic can be used to identify the element whose distribution is revealed by the autoradiograph. The half-period is determined from the rate of decrease in the activity when the mineral specimen is placed in front of a beta-ray counter. For most samples the background of the counter is negligible, being only about 100 counts per minute as compared to several thousand per minute for an average induced activity. When the background is appreciable, the rate of decrease must of necessity be based on the net activity due to the sample alone. If two or three elements contribute simultaneously to the activity, these can often be resolved if the half-periods are substantially different and the decay measurements are made over an extended period of time. Occasionally two elements of nearly the same half-period are present, in which case it may not be possible to distinguish between them. However, even in these instances, activation by neutrons of selected energies may help identify individual elements if resonance levels exist in the nuclei.

Experimental Results

For reconnaissance purposes nine elements of general interest to geologists were selected for special study, namely: manganese, gold, copper, tungsten, phosphorus, potassium, barium, sodium, and arsenic. The distribution of these elements in various mineral specimens is revealed in the prints of the autoradiographs, Figs 2–11 inclusive. Experimental and expected decay curves drawn on arbitrary scales are also included, together with direct photographs of each mineral. In addition, the pertinent nuclear properties of all the elements have been compiled to determine their suitability and characteristic reactions. Out of 41 elements for which relatively complete data are available,† at least 26 should be suitable for autoradiography, if present in high concentrations. It is, of course, desirable that common "gangue" elements have little or no activity, so that they will not interfere. Fortunately, this was found to be true of iron, sulphur and oxygen, and to a lesser degree of aluminum and silicon.

Luminescence was observed in most of the specimens known to fluoresce in ultraviolet light This effect was first observed in a scheelite specimen whose autoradiograph is not included. Tests were made on this and other specimens by separating portions of each from the photographic film with black paper and with cellophane. The paper and cellophane absorb the beta radiation to about the same degree, but visible light is completely absorbed by the black paper and is not appreciably affected by the cellophane. For the luminescent specimens, greater darkening is found below the cellophane than below the paper. After this effect had been discovered photographically, it was found that the light was visible in the dark after the eyes had become adapted.[4]

While luminescence does not interfere with the determination of the locus of the active element in a specimen, it does interfere with an estimate of the relative concentration. For example, in Fig. 10, the willemite, because of its luminescence, gives a brighter area in the print than the franklinite, although it actually contains less manganese than the franklinite.

PHOTOGRAPHY

Although all photographic materials are affected by nuclear radiations, films differ greatly in their sensitivity. This sensitivity may or may not be related to the sensitivity to ordinary light. For use with beta rays, the Eastman Kodak Company recommended medium lantern-slide plates and high-resolution 548 plates with blue sensitizing. In addition to these materials, tests were made of a number of other plates and films, including *x*-ray films. The sensitivity of most of these, including the 548 plates, was so low that even the highest beta activities produced little effect. On the other hand, the *x*-ray films are quite sensitive, as would be expected. Although considerably less sensitive than the x-ray films, the lantern slides have moderate sensitivity to beta rays and give much finer grain and hence greater detail than the x-ray films. For this reason, medium lantern slides are recommended except when the highest sensitivity is needed.

---

† These data have been arranged in a periodic table of the elements, copies of which are available without charge on request.

[4] Subsequently we learned that F. G. Wick and M. S. Vincent, *Phys. Rev.*, **58**, 578 (1940), observed luminescence in certain phosphors during exposure to neutrons. However, these investigators apparently did not have a sufficiently intense source of neutrons to induce the persistent luminescence herein reported.

The resolving power of the autoradiographic method is limited by (1) the grain size of the film or plate, (2) the blurring effect of rays from below the surface of the specimen, and (3) the geometrical distribution of the radiation. Grain size has been considered in the preceding paragraph. The blurring effect is not as serious as might at first be expected, since only the highest-energy beta rays can penetrate from depths as great as 1 mm. in the specimen. Because the rays are emitted equally in all directions, a cone of blackening from each active point in or near the surface of the specimen is produced in the film. This is equivalent to having the image slightly out of focus. The magnitude of these effects is indicated in the accompanying figures.

ACKNOWLEDGMENTS

The authors are indebted to the members of the Radioactivity Center for their assistance and suggestions during this work. In particular, the cooperation of the M.I.T. cyclotron group, in providing an intense source of neutrons, and of Dr. J. W. Irvine, Jr., in permitting the use of his counter apparatus, is gratefully acknowledged. Professor L. C. Graton has been most generous in his encouragement and interest. Professors W. H. Newhouse and A. M. Gaudin provided all of the samples and offered valued criticism. Mr. E. P. Kaiser aided in the identification of willemite in one of the specimens. The more recent developments of this research have been made possible by a grant-in-aid from the American Academy of Arts and Sciences.

FIGURES 2–10, AUTORADIOGRAPHS, PHOTOGRAPHS AND DECAY CURVES

A print of a direct photograph is shown in the upper left corner of each figure. The corresponding autoradiographic print of the same surface, reduced to the same scale, is shown immediately below. The experimentally observed radioactivity decay curve (solid line) is shown graphically on the right, the β activity being in arbitrary units. The slope of the curve is proportional to the half-period. For comparison the expected value for the element indicated is shown as a broken line.

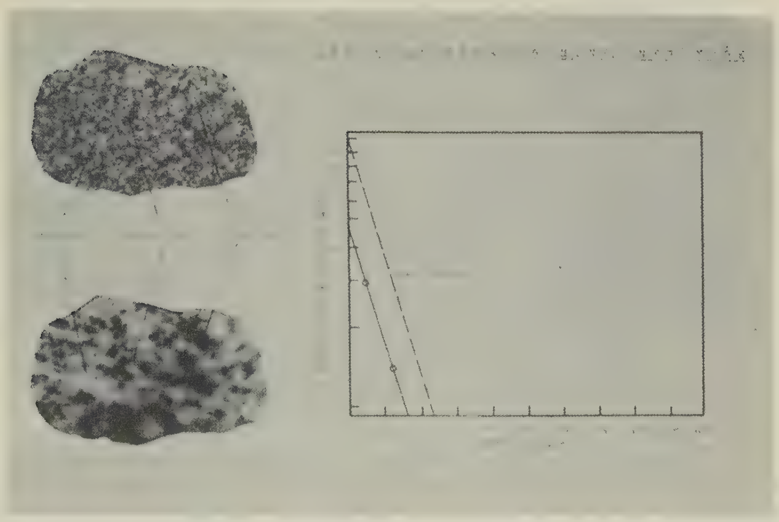

FIG. 2. Zinc ore from Edwards Mine, New York, shows high activity, possibly of barium, in calcite, intermediate activity in sphalerite and essentially no activity in pyrite.

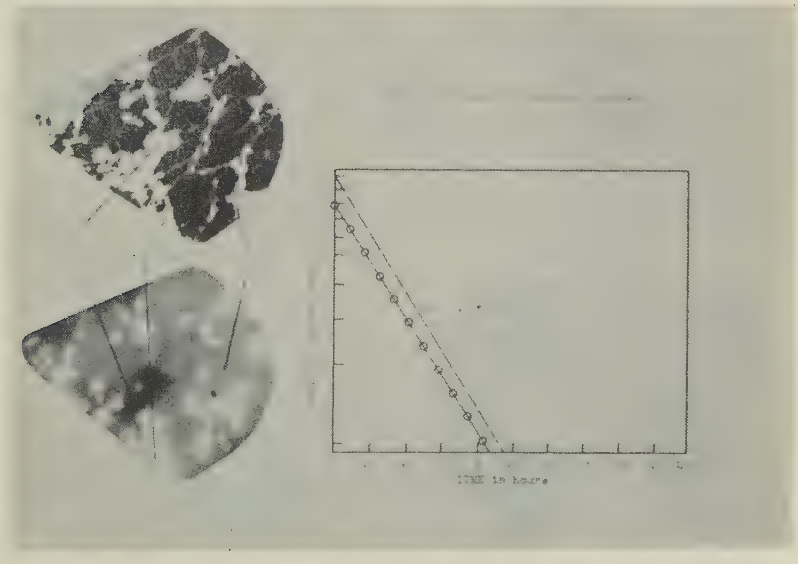

FIG. 3. Norwegian magnetite ore shows apparent high activity of manganese in calcite, moderate activity in magnetite and none in quartz.

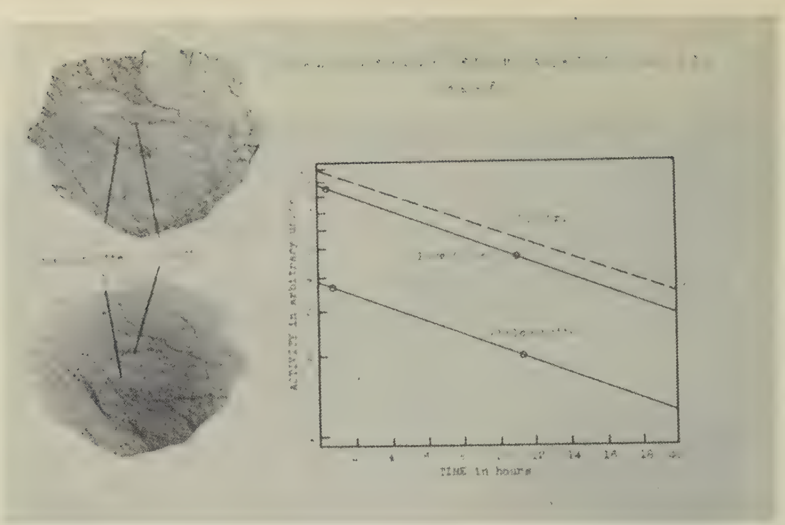

FIG. 4. Chalcopyrite from Amador County, California, shows expected uniform distribution of copper in mineral with exception of quartz stringers. Activity of pure copper was determined under similar conditions in an attempt to test quantitative application of method. Theoretical Cu content is 35 per cent, while curves indicate 43 per cent, suggesting possible greater absorption of β-rays in copper than in chalcopyrite.

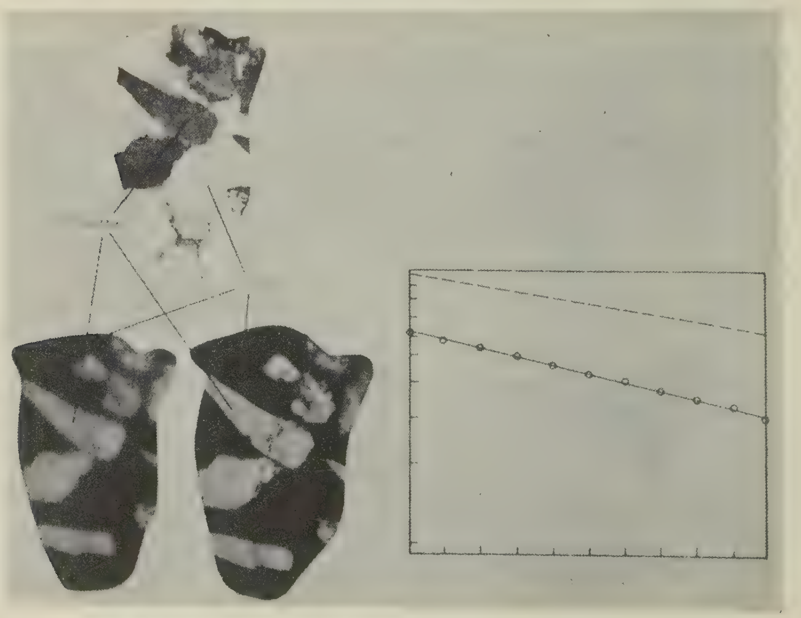

FIG. 5. Two autoradiographs of a Spanish tungsten ore were obtained. The first, lower left, made immediately after activation, reveals the distribution of manganese in the wolframite. The quartz shows no activity. After the manganese activity (half-period 2.6 h.) had practically all decayed, the second autoradiograph, showing the distribution of tungsten, was made. The decay curve observed 24 hours after bombardment has a slightly steeper slope than that of tungsten alone, presumably due to some contribution from manganese.

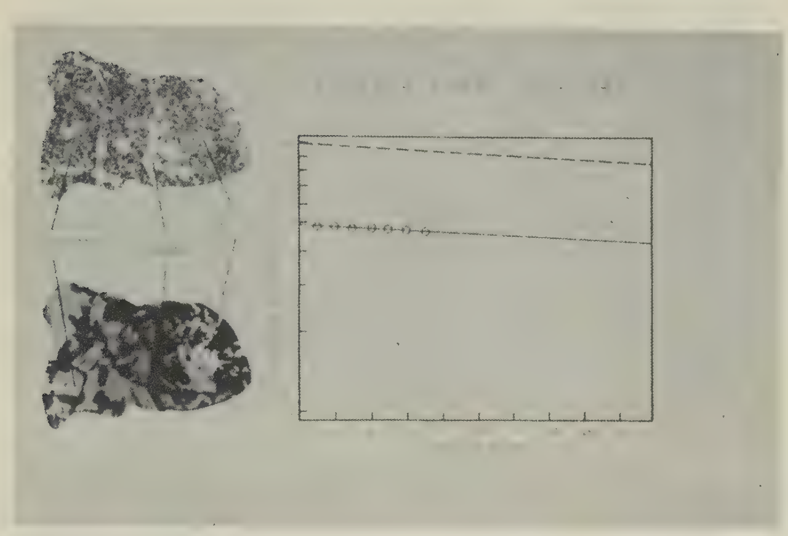

FIG. 6. The presence of native gold in the Cripple Creek gold ore is indicated by bright areas in the autoradiograph. The gray areas correspond to calaverite which has a lower gold content. Again the quartz shows no activity.

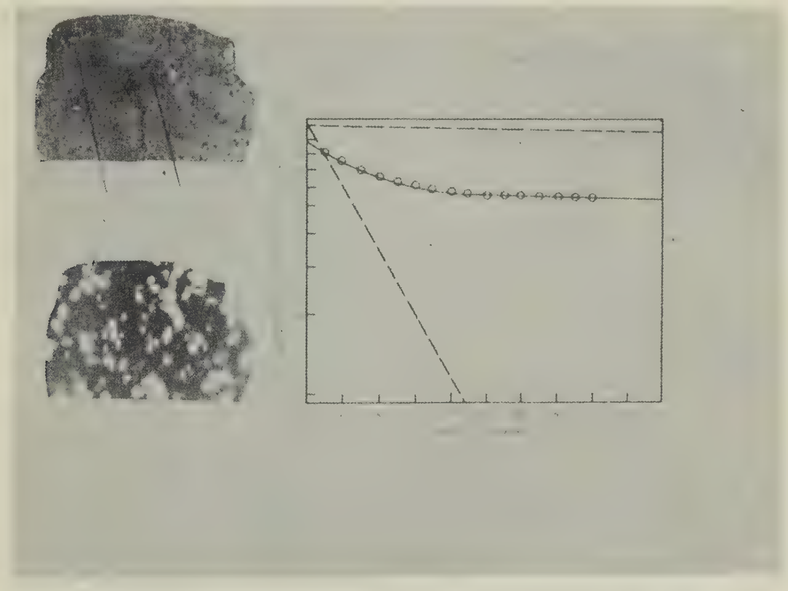

FIG. 7. A sharp contrast is shown between the apatite and the magnetite. Unlike the magnetite in the Norwegian ore of Fig. 3, this magnetite shows essentially no activity, indicating a relatively low concentration of manganese. The steeper slope in the early part of the decay curve suggests that the apatite is manganiferous. After the manganese activity has died away, the slope parallels that of phosphorus (half-period 14.5 d.).

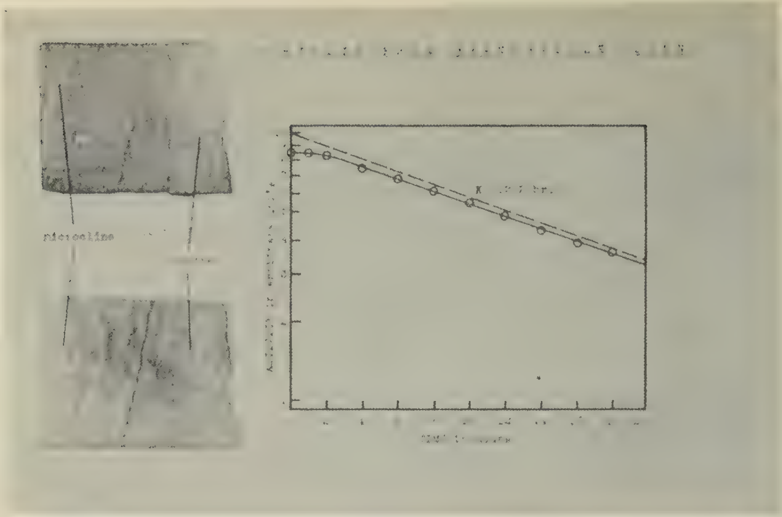

FIG. 8. After activation the microcline in a perthite from Branchville, Conn., produced a greater photographic effect than the associated albite. At first this seemed surprising, since potassium has a somewhat smaller capture cross-section than sodium (see Table 1) and both are present in approximately the same atomic concentration. Upon further study it was found that the microcline was luminescent following activation. Because of the similarity in the half-periods (Na, 14.8 h.; K, 12.2 h.), it was not possible to distinguish between these two elements in the decay curve, and sodium may have contributed as much or even slightly more to the total β activity than potassium.

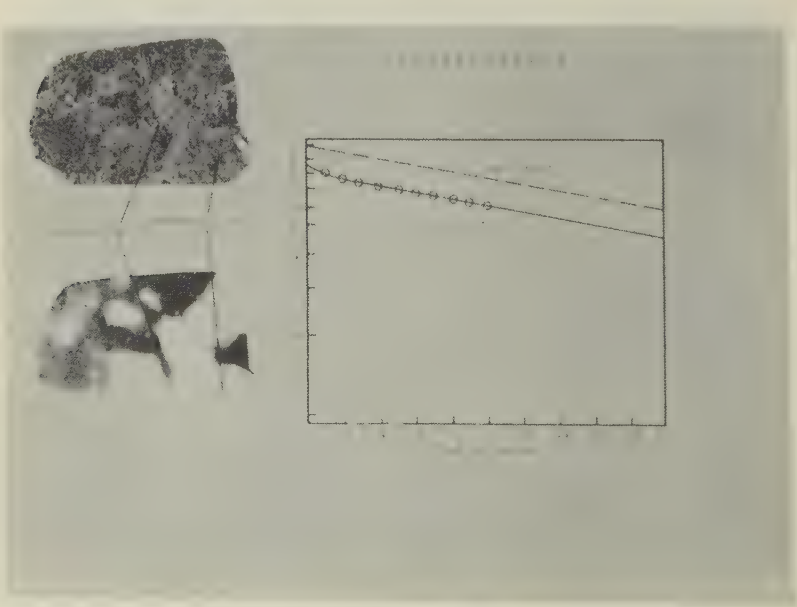

FIG. 9. In the autoradiograph the arsenopyrite crystals do not show a sharp boundary with the adjacent chalcopyrite. This effect is due to the predominance of γ over β radiation in activated arsenic. Since the γ-rays are much more penetrating and have an indefinite range, their autoradiographic effect is much more diffuse. The decay curve was obtained with 1 mm. of lead between the sample and the counter, hence it indicates the decay of the γ radiation.

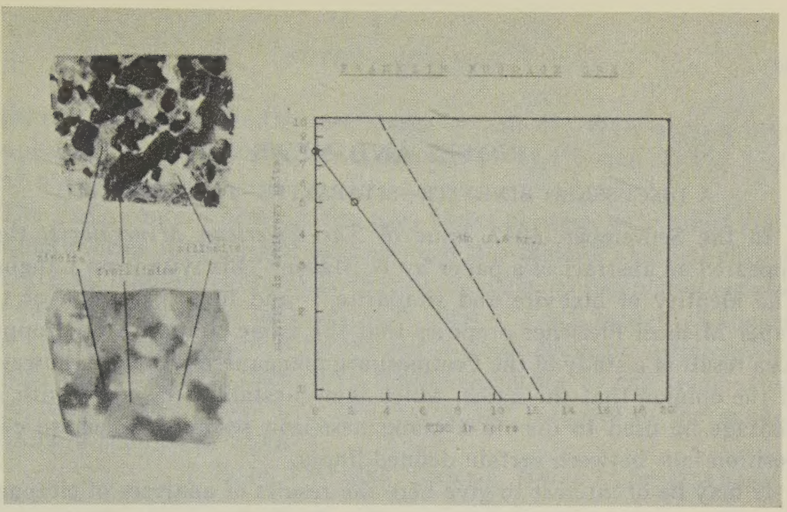

FIG. 10. Because of its luminescence, the willemite in the Franklin Furnace ore produced a distinctly darker area in the autoradiograph, hence a brighter area in the print, than the associated franklinite even though the latter is known to contain a substantially higher manganese content. The zincite showed essentially no activity. An inadequate decay curve was obtained for this sample.

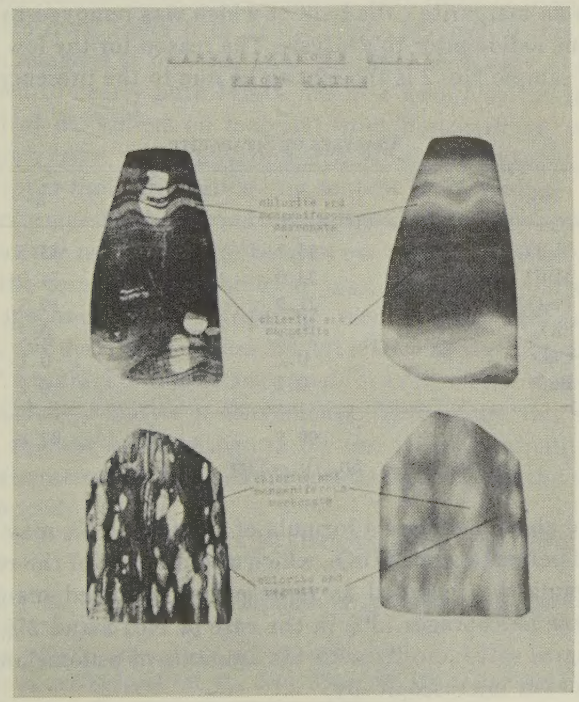

FIG. 11. The autoradiographs of two samples of manganiferous shale from Maine are shown on the right with corresponding direct photographs on the left. The light blotches in the upper left are etch marks on the polished surface. The striking localization of the more manganiferous material in certain laminae and nodules is clearly shown. These observations are of interest in the beneficiation of the ore.

NOTES AND NEWS

A DISCUSSION: BIXBYITE—SITAPARITE—PARTRIDGEITE

In the September, 1942, issue of *The American Mineralogist* there appeared an abstract of a paper by B. Mason: "Bixbyite from Långban. The identity of bixbyite and sitaparite,"[1] and in a discussion of this paper Michael Fleischer proposes that the name sitaparite be dropped. As a result of a study of the Postmasburg manganese ores I am, however, of the opinion that the name, which is well-established, could with advantage be used to denote a manganese-iron sesquioxide whose composition falls between certain defined limits.

It may be of interest to give here the results of analyses of sitaparite from Postmasburg, carried out by Dr. C. F. J. van der Walt of the Division of Chemical Services. The analyzed specimens were polished on three sides and the amounts of the impurities (psilomelane and pyrolusite) estimated by inspection under the reflecting microscope. In the case of sample No. 1 these were judged at 1% and in the case of sample No. 2 at 2%. The latter contained in addition a fair percentage of ephesite (soda margarite), the bulk of which was removed by separation in methylene iodide prior to analysis. The reason for the low total of the analysis of sample No. 2 is thought to be due to the presence of residual ephesite.

Analyses of Sitaparite

No.	1	2
MnO_2	44.2	43.5
MnO	33.0	34.0
Fe_2O_3	21.9	19.3
SiO_2	0.1	0.5
CaO	0.2	0.1
BaO	0.1	0.2
	99.5	97.6
	Sp. Gr. = 5.00	

From the above analyses a formula of the type R_2O_3 may be deduced if the small percentages of MnO_2, which are in excess of the requirements of the formula, be regarded as representing admixed manganese peroxides. These percentages (3% in the case of No. 1 and 2% in the case of No. 2) agree satisfactorily with the amounts of psilomelane and pyrolusite estimated microscopically.

---

[1] *Geol. Fören. Förhandl.*, **64**, 117–125 (1942).

Determinations of Fe_2O_3 were made by van der Walt on two other samples of fairly pure sitaparite. Results of 14.4% and 25.6% Fe_2O_3 were obtained.

The Fe_2O_3 content of sitaparite thus varies between wide limits and a complete series apparently exists between this mineral and bixbyite. As the original bixbyite contains 47.98% Fe_2O_3, a logical distinction between the two minerals could be made on a basis of Fe_2O_3 content. I suggest that the name partridgeite[2] be applied to those manganese-iron sesquioxides containing less than 10% Fe_2O_3, sitaparite to the sesquioxides containing between 10% and 30% Fe_2O_3, and bixbyite to the mineral with more than 30% Fe_2O_3.

J. E. de Villiers, *Pretoria, Union of South Africa.*

It has been known for some years[3] that pure Mn_2O_3 has the same crystal structure as the mineral bixbyite, $(Mn,Fe)_2O_3$. It would have been reasonable to expect that naturally occurring material would show the entire range of composition. However, all the analyses of bixbyite until recently were made on material of pneumatolytic origin and all were very high (42–59%) in Fe_2O_3 content. Very recently Mason[4] showed that sitaparite from India with 27.6% Fe_2O_3 belongs to this series and also gave an analysis of material from Långban with only 21.9% Fe_2O_3. The gap down to nearly pure Mn_2O_3 has now been filled by the work of Gruner[5] and of de Villiers on material from Postmasburg, so that the series is known from essentially iron-free Mn_2O_3 to material with 59% Fe_2O_3. The upper limit of possible iron content is not known.

De Villiers suggests that three names be used for the series. Mason proposed that the name bixbyite be used for the entire series. He wrote: ". . . then the mineral name bixbyite may be defined precisely as including all specimens with manganese, iron, and oxygen as principal components, and having the same crystal lattice as the original bixbyite from Utah." Arguments can be advanced for both views. It seems to the writer to be chiefly a matter of convenience. As there are only six verified occurrences, the use of three names for the series seems to be an unnecessary elaboration. It is therefore recommended that the name sitaparite be dropped.

Michael Fleischer, *U. S. Geological Survey.*

---

[2] De Villiers, J. E., A preliminary description of the new mineral, partridgeite: *Am. Mineral.*, **28**, 336–338 (1943).

[3] Zachariasen, William, *Zeits. Krist.*, **67**, 455–401 (1928).
Pauling, Linus, and Shappell, M. D., *Zeits. Krist.*, **75**, 128–142 (1930).

[4] Mason, Brian, *Geol. För. Förh.*, **64**, 117–125 (1942).

[5] Gruner, J. W., *Am. Mineral.*, **28**, 174 (1943).

NOMINATIONS FOR OFFICERS OF THE MINERALOGICAL SOCIETY OF AMERICA FOR 1944

The Council has nominated the following for officers of the Mineralogical Society of America for the year 1944:

PRESIDENT: R. C. Emmons, University of Wisconsin, Madison, Wisconsin.
VICE-PRESIDENT: H. Berman, Harvard University, Cambridge, Massachusetts.
SECRETARY: Paul F. Kerr, Columbia University, New York, N. Y.
TREASURER: Earl Ingerson, Geophysical Laboratory, Washington, D. C.
COUNCILOR (1944–47): S. J. Shand, Columbia University, New York, N. Y.

Following the decision of the Geological Society of America, there will be no annual meeting of the society during 1943. Members of the society who wish to may submit abstracts of scientific papers to be published in the March–April 1944 issue of the *American Mineralogist.* As usual, the ballots for officers of the society and for candidates for fellowship will be sent out from the Secretary's office approximately October 10.

PAUL F. KERR, *Secretary*

RULES FOR THE CONVENTIONAL ORIENTATION OF CRYSTALS: A CORRECTION

J. D. H. DONNAY, *Hercules Powder Company, Wilmington, Delaware.*

The space group of lorandite in the Peacock setting (*Am. Mineral.*, **28**, 326, 1943) was represented by $P2/x$, with glide-component $\frac{1}{2}(\mathbf{a}+2\mathbf{c})$, and the criterion for the zone $[(h0l)]$ was expressed as "$(h+2l)$ even." As Dr. M. J. Buerger kindly pointed out to me, this method of symbolizing the space group is unnecessarily complicated. It is equivalent to the simpler notation $P2/a$ (with criterion "h even"), for a glide-component $\frac{1}{2}\mathbf{a}$ has the same effect as a glide-component $\frac{1}{2}(\mathbf{a}+2\mathbf{c})$.

Erratum

Page 319, first line, read "to discard the $\alpha\beta$ rule . . . etc."

Correction

In *The American Mineralogist*, **28**, 214 (1943), illite was listed among discredited species with the statement illite = bravaisite. A paper by R. E. Grim and R. A. Rowland was cited as authority. Dr. Grim has kindly pointed out that this was a misinterpretation of his views and has suggested that the usage involved should be clarified.

Illite is not the name of a specific mineral species. It should be used only as a *general term* for the clay mineral constituents of argillaceous sediments belonging to the mica group. The exact nature of these mica-like clay mineral constituents is as yet uncertain, but the evidence thus far obtained seems to indicate that the dominant *specific species* present is bravaisite, in some occurrences associated with more or less montmorillonite.

MICHAEL FLEISCHER